Master of Science Thesis
HT2021

Environmental radiation measurements at Barsebäck nuclear power plant during the decommissioning phase

Patrik Dahlström

Supervisors

Christian Bernhardsson, Ünal Ören, Mattias Jönsson, Malmö

This work has been conducted at
the Medical Radiation Physics,Malmö

π

Medical Radiation Physics, Lund
Faculty of Science
Lund University
www.msf.lu.se

Radiologisk karakterisering av Barsebäck kärnkraftverks närmiljö

Barsebäcks kärnkraftverk driftsattes 1975 och den första reaktorn togs ur drift 1999 och den andra 2005. Nedmontering och rivning av kärnkraftverket har inletts och processen beräknas vara klar på 2030-talet. Syftet med detta examensarbete är att kartlägga eventuell radioaktiv kontamination i området runt Barsebäcksverket. Mitt mål är att ta fram en metod för att särskilja bakgrundsstrålning från antropogena radioaktiva ämnen, *dvs*. radioaktiva ämnen producerade genom mänsklig interaktion med naturen såsom vid kärnvapensprängningar och drift av kärnkraftverk. Av särskilt intresse är antropogena radionuklider som härrör från Barsebäcksverkets aktiva tid likväl dess nedmontering och rivning. I omgivningen kring Barsebäcksverket finns framförallt två sådana intressanta gammaemitterande radionuklider, cesium-137 (^{137}Cs) och kobolt-60 (^{60}Co) som är av betydelse när området så småningom ska friklassas. För denna kartläggning användes ett antal olika mätinstrument och mätmetoder som kan detektera och kvantifiera radioaktiva ämnen och strålning. Aktivitetskoncentrationen kvantifieras med jordprover och fältmätning, så kallat *in situ* gammaspektrometri. Båda metoderna använder en germaniumkristall (HPGe) halvledardetektor som mäter energifördelningen hos gammafotoner vilka emitteras från jordprovet respektive marken vid *in situ* gammaspektrometri. Aktivitetskoncentrationen hos samtliga radionuclider mäts i Bq/kg för jordprover medan ute i fält enbart naturligt förekommande radionuklider mäts i Bq/kg, medan antropogena radionuklider mäts i termer av Bq/m^2. Utöver dessa metoder utfördes *in situ* mätningar med en spektrometer-dosimeter vilken ger aktivitetskoncentrationen för naturligt förekommande radionuklider samt miljödosekvivalent doshastighet. Med dessa värden är det möjligt att beräkna antropogena radionukliders bidrag till doshastigheten. Doshastighetsmätning utfördes även med ett doshastighetsinstrument för att beräkna ett medelvärde av doshastigheten i ett visst område. För radiologisk kartläggning av ett större område användes mobil gammaspektrometri, som kan utföras på många olika sätt. Till exempel kan man vandra med ryggsäck som innehåller en spektrometer kopplad till GPS och en bärbar dator. Det möjliggör att man kan studera doshastigheten i olika koordinater, vilket är användbart för att lokalisera områden med förhöjd radioaktivitet. Mobil gammaspektrometri genomfördes också med en specialutrustad bil som innehåller detektorer och på samma sätt som nämns ovan läser av doshastigheten och koordinater. Ett urval av 10 platser valdes för att utföra noggranna mätningar, där ingick 4 platser utanför kärnkraftverkets område samt 6 platser innanför området. Mätningarna visade svagt förhöjda nivåer av antropogena radionuklider på ett fåtal platser. Dessa var belägna innanför stängslet, i två dammar samt på ett område bredvid dammarna. I övrigt visade mätningarna att inga signifikanta spår från driften syns och aktivitet från antropogena radionuklider ej översteg de normala bakgrundsnivåer från Tjernobylolyckan (1986) och de atmosfäriska kärnvapentester (1950- och 1960-talet).

LUND UNIVERSITY

Abstract

Faculty of Science
Medical Radiation Physics

Environmental radiation measurements at Barsebäck nuclear power plant during the decommissioning phase

by Patrik Dahlström

Background and aim: The Barsebäck nuclear power plant (NPP) units ceased operations in 1999 and 2005. Now the NPP is in the phase of decommissioning, which is a complicated process that will take many years to complete. Radiological characterization of the surrounding area is a part of the decommissioning process. The aim of this thesis was to identify and quantify residual anthropogenic radioactivity at the site area, by selecting a number of locations around the NPP and carrying out different radiological measurements and then analysing the result. Radionuclides of interest were anthropogenic gamma emitting nuclides such as ^{137}Cs and ^{60}Co that are related to NPP activities.
Method: Measurements were carried out at 10 sites around the NPP area. Each site was measured with *in situ* gamma spectrometry using a HPGe detector to assess the gamma emitting radionuclides. Dose rate was determined with a handheld dose rate meter. Soil samples were collected to determine the activity concentration of gamma emitting radionuclides at different depths of the soil. A spectrometer-dosimeter was used to assess the contribution of anthropogenic radionuclides to the dose rate. Mobile gamma spectrometry was carried out in the area to achieve a radiological coverage of larger areas than the *in situ* measurements. Additional measurements were made to cover other areas as well, *i.e.* the restricted area of the NPP. A $LaBr_3$ scintillation detector positioned in a backpack was used to perform mobile gamma spectrometry on foot. Radioactivity along the roads were mapped by a car-borne system consisted of two large volume NaI(Tl) scintillation detectors.
Results: ^{137}Cs was detected at all measurement points with *in situ* gamma spectrometry, where the highest levels were found at site 9 and 10 (569 Bq/m^2 and 719 Bq/m^2). The majority of the ^{137}Cs contamination are residues from the Chernobyl accident and nuclear weapon tests. ^{60}Co was also detected at a few sites with *in situ* gamma spectrometry, where the highest values were found at site 8, 9 and 10 (65 Bq/m^2, 67 Bq/m^2 and 79 Bq/m^2). However, it should be emphasized that as a general trend the ^{60}Co activity concentrations were relatively low and that ^{60}Co was only detected in one of the soil samples. Activity concentration of ^{137}Cs in soil samples were at most 14.7 Bq/kg. Site 8 and 10 had elevated levels according to previous studies of these particular sites. Dose rate measurements at sites 1-10 showed no indication of significant increase in dose rate and resembled background radiation ($\sim$100 nSv/h), typical for the region. The backpack mobile gamma spectrometry did not distinguish any increases of dose rate above background at and around sites 1-10. However, inside the restricted area there were several sites with increased radiation levels, above the natural background. These elevated levels are, however, attributed to different building structures in the area. The car-borne measurements also discovered a few areas where the radiation levels were elevated. The spectrometer-dosimeter measurements showed the largest contribution from anthropogenic radionuclides at sites 8 and 10 (25% and 26%).
Conclusion: Anthropogenic radionuclides were detected in the surroundings of the Barsebäck NPP, both inside and outside of the industrial area. The observed results for ^{137}Cs are comparable to other areas in Skåne. Sites closer to the contaminated ponds contained more ^{60}Co than sites further away from the ponds, with the highest levels found at sites 8, 9 and 10. The radioactivity in the ponds originate from previous dredging activities where contaminated sediments were placed in the two ponds. The activity concentrations of ^{60}Co were below minimum detectable activity (MDA) in the soil samples. The results of the thesis can be used as a reference for the future site clearance and constitute a basis for future investigations.

Acknowledgements

Thanks to my supervisors for helping me this semester. Christian Bernhardsson, for handing me relevant information sources and guiding me in my work. Ünal Ören, for providing me with reports concerning Barsebäck NPP and being of constant help at the NPP. Mattias Jönsson, for providing help with the equipment and helping me with data analysis. Thank you all for sharing your expertise and guiding me in the right direction.

I would also like to express my gratitude towards the whole group at Barsebäck nuclear power plant who were welcoming and helpful, providing interesting talks and sources of information.

To my family and friends I would like to thank you for supporting me in my work and studies.

Contents

List of Figures

List of Tables

List of Abbreviations

NPP	**N**uclear **P**ower **P**lant
ADER	**A**mbient **D**ose **E**quivalent **R**ate
NORM	**N**aturally **O**ccurring **R**adioactive **M**aterials
MDA	**M**inimum **D**etectable **A**ctivity
HPGe	**H**igh **P**urity **Ge**rmanium
NaI(Tl)	Sodium Iodide doped with Thallium
LaBr	**La**nthanum **Br**omide
ROI	**R**egion **O**f **I**nterest
GM	**G**eiger **M**üller
MCA	**M**ulti **C**hannel **A**nalyzer
ESS	**E**uropean **S**pallation **S**ource
DU	**D**etection **U**nit
IPU	**I**nformation **P**rocessing **U**nit
KCl	Potassium Chloride
NIST	**N**ational **I**nstitute of **S**tandards and **T**echnology
IAEA	**I**nternational **A**tomic **E**nergy **A**gency
SSM	Swedish Radiation Safety Authority
CC	**C**onversion **C**oefficient
ADC	**A**nalog to **D**igital **C**onverter

Chapter 1

Background and aim

The aim of this master thesis is to examine whether or not the area around the Barsebäck nuclear power plant (NPP) contain radioactive contamination that can be traced to the days when it was in operation. Furthermore, it is of interest to qualitatively assess the origin of the contamination as well as the quantity of the contamination. The power plant has been completely shut down, where reactor B1 ceased operation in 1999 and reactor B2 in 2005. Approval for dismantling was granted by the regulator in 2020 and the NPP is currently being dismantled part by part. The decommissioning process for a NPP is a project that takes many years to complete. Not only does decommissioning of a NPP require demolition of buildings after these are subjected to clearance but it also requires waste management and decontamination of equipment and materials that have been contaminated with radioactivity. In theory, the radioactive contamination will subside in time and eventually there will be small levels of activity left. However, in practice it is not possible to do this since some radionuclides have a long half-life. It is also of importance that the dismantling process is performed in a careful and planned manner so that there is as little discharge of radioactivity to the surrounding environment as possible. Airborne contamination from decommissioning of the NPP can be produced and easily spread in the form of aerosol particles and gases when cutting materials or demolishing building materials. Decommissioning of the Barsebäck NPP is currently (end of 2021) in a stage where the exterior buildings are still intact and where dismantling of different type of components is ongoing. Some of the activated reactor materials and other contaminated materials and equipment are temporarily stored in customized interim storages, until they can be moved to the final repository.

Regardless if the future site use will be restricted or unrestricted when the decommissioning process is completed, it is important that the radioactivity levels are below the dose limit set by the authority. Thus, in order for the area to become available, the ground has to be evaluated for its radioactivity concentration. With the use of a method called radiological characterization the ground can be measured for radioactivity through soil samples and measurement with *in situ* gamma spectrometry. The aim was to perform measurements in strategically selected locations that allowed for a good coverage of the area. In these locations, or sites, different methods of radioactivity measurements were used, such as *in situ* gamma spectrometry. Obtaining a reasonable amount of soil samples from each site also helped in representing the true activity concentration in each respective site. In addition, a large area of each site were covered with mobile gamma spectrometry by car or backpack measurements. On each site the radiation exposure was also measured using a handheld dose rate instrument displaying ambient dose equivalent rate (ADER). Furthermore, the objective was also to determine the quantity

of the total ADER that originates from contamination due to the operation of the NPP and other anthropogenic sources. For that purpose, a spectrometer-dosimeter equipped with a NaI(Tl) scintillation crystal was used.

Chapter 2

Theory

The ground around the Barsebäck NPP contain radionuclides just like any other ground on this planet. The soil contains naturally occurring radioactive materials (NORM). In addition to NORM it is also, although very little, contaminated with radionuclides from external anthropogenic sources that have spread to this location. Over time, the number of anthropogenic radionuclides in contaminated areas will decrease, due to many of the anthropogenic radionuclides having short half-life. The deposition of gamma emitting anthropogenic radionuclides at the terrestrial and aquatic environment around the NPP now consist primarily of ^{137}Cs (fission product) and ^{60}Co, where the latter is produced from activation of materials originating from Barsebäck NPP. ^{137}Cs detected at the site is mainly from the Chernobyl accident and the atmospheric nuclear weapon tests conducted in the 1950s and 1960s.

2.1 Decommissioning process of a NPP

The decommissioning of a NPP generally consists of seven steps according to the Swedish Radiation Safety Authority (SSM)[1]. Prior to building and commissioning a NPP, planning for future decommissioning is necessary and certain aspects has to be considered, such as waste management *etc.* In Figure 1 these steps are summarized.
1) The first executive step towards decommissioning is taken during the time that the NPP is still in operation. At this time, planning of such is intensified.
2) Permanent shutdown of electricity production at the NPP mark the next stage of decommissioning.
3) In the transition phase preparations are made to dismantle the reactor where radiation safety is emphasized. Spent nuclear fuel is extracted from the reactor and transported to a dedicated interim storage facility. Reactor systems are then decontaminated using for example chemical methods to remove the radioactive contamination, to minimize the radiation exposure to workers. During this phase systematic measurements are performed to characterize potential radiation sources

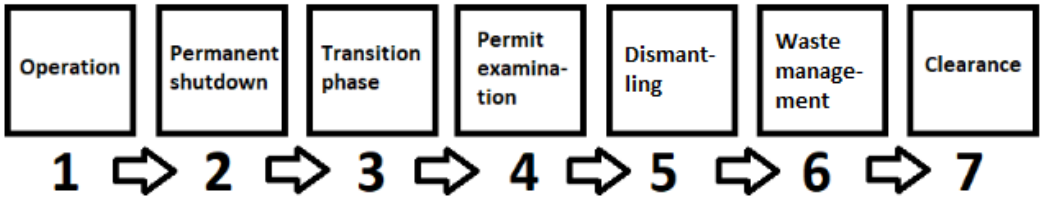

Figure 1: NPP decommissioning step by step according to SSM.

in the facility.
4) Before decommissioning can be initiated a permit examination must be passed in accordance with the environmental code. SSM also have to give their approval in order to proceed with the process.
5) Granted these permits are given, the decommissioning can begin with dismantling installed systems and sorting them into categories of radioactively contaminated materials and conventional materials.
6) Contaminated building surfaces and materials are decontaminated in an attempt to remove the radioactivity. Buildings with no future purpose are demolished after clearance and the ground is surveyed for contamination. Possible contaminated areas are then subject to remediation measures.
7) The ultimate goal of decommissioning is clearance of the site. Clearance is reached in the final step when the remaining radioactivity contribution in the ground is below clearance levels.

The site can be categorized according to the risk for contamination as described by the Swedish Nuclear Fuel and Waste Management (SKB) guidelines[2]. There are four categories to separate areas of different radioactive contamination levels and these are areas with extremely small risk, small risk, risk and radioactive contamination above the clearance level. If the area is contaminated the clearance criteria must be met before it can be used for other purposes. The area could be subject to both unconditional and conditional clearance depending on the future reuse scenario. When there is a restriction of the use for the area it is called conditional clearance. Such a restriction may involve an industrial area where some dose contribution to individuals from exposure pathways such as cultivation of crops and livestock for consumption are unlikely to occur. The unrestricted clearance scenario takes into account all possible exposure pathways, such as ingestion of plants, meat and milk produced at the site. The true purpose of clearance is to uphold health and safety of the public, minimizing the exposure risk from residual radioactivity by making sure that radioactivity is contained and supervised in a secure manner away from the general public.

2.2 Naturally occurring radioactive materials

Radioactivity is present everywhere in the ground of the earth as it contains NORM radionuclides, and has been radioactive since the formation of earth. It constitutes many radionuclides, with a basis of ^{40}K, ^{235}U, ^{238}U and ^{232}Th. The uranium and thorium components are primordial in their respective decay chains which are called the actinium-, uranium- and thorium series respectively. There used to be a neptunium series as well, however, only ^{209}Bi remains of the series due to the relatively short half-life of its primordial radionuclide ^{237}Np. From each primordial radionuclide there are many radioactive daughter nuclei that follows in series from their decay. Hence the ground is composed of all of these elements as well. Other radionuclides that occur naturally are ^{14}C and ^{7}Be, both cosmogenic and produced from nuclear reaction between high energy particles and oxygen and nitrogen, respectively, which are both present in air and environment. Long measurement of NORM is needed to be able to achieve statistically satisfying result due to low activity concentrations. Difficulties in quantifying the radioactivity of certain NORM radionuclides is that some radionuclides emit similar energy leading to spectral interference. It is thus important to have knowledge of the decay

chains when analysing a NORM spectrum.

During secular equilibrium of the uranium series, some daughters are easier to determine from a gamma spectrum than others in gamma spectrometry (gamma spectrometry as a detection method of gamma ray emitting radionuclides is discussed in a later section), in particular ^{234}Th, ^{234m}Pa, ^{226}Ra, ^{214}Pb, ^{214}Bi and ^{210}Pb. Secular equilibrium is due to the parent nuclei having a much longer half-life than its daughters without interruptions or disturbances. During secular equilibrium the activity of the daughter is equal to the parent activity thus enabling quantification, which typically occurs after five half-lifes of the daughter nuclei.

^{238}U comprise 99.25% of the total uranium supply in the ground while ^{235}U comprise only 0.72%. However, the significance of ^{235}U in the energy spectrum is comparable to ^{238}U even though it represents such a small fraction of the total uranium in the ground. The reason for this is the shorter half-life of ^{235}U. Daughter nuclides of the ^{235}U decay chain are difficult to measure but with some effort ^{227}Th, ^{223}Ra and ^{219}Rn can be measured. However the easiest way to analyse the ^{235}U decay chain is to measure ^{235}U through gamma spectrometry. ^{235}U major gamma energy is similar to the gamma energy of ^{226}Ra, both at around 186 keV, leading to mutual spectral interference[3].

Spectral interference occur due to two radionuclides emitting similar energies, resulting in errors when calculating the activity of one or the other. A solution to this problem is to remove interfering radionuclides through a separate (background) measurement, without the radionuclides of interest present. Potassium, thorium and uranium will always cause spectrum interference in background measurements, hence peaked background correction is a useful tool when assessing the activity of radionuclides.

One thing to note about the actinium series is that the gamma radiation contribution is very low in comparison to the uranium- and thorium series[4, 5]. Thorium series primordial radionuclide is ^{232}Th where four radionuclide daughters in the series are easily measured with gamma spectrometry, ^{228}Ac, ^{212}Pb, ^{212}Bi and ^{208}Tl.

All decay chains contain a radon isotope which is a gaseous radionuclide. This gaseous trait enable the radionuclide to escape and thereby disturb the equilibrium of the decay chain. This can be problematic when doing measurements since such disturbance lead to a change in activity for daughter nuclides of radon. For actinium- and thorium series this is not much of an issue since the half-life of their respective radon isotopes are short (4 s and 56 s). But in the uranium series the radon isotopes has a half-life of 4 days and hence the return to equilibrium takes much more time. In general, it takes about ten half-lives of the missing radionuclide to reestablish equilibrium.

Gamma spectrometry performed in an outdoor environment without contribution of anthropogenic radionuclides generate a background spectrum where only NORM and cosmic radiation is present. In such background spectrum the ^{40}K peak at 1461 keV is often the most prominent peak. ^{40}K is present in *e.g.* soil, wood and building materials, living organisms as well as in the human body. This means that each human being is radioactive, generating an internal dose of about 0.2

mSv/year from ^{40}K alone[6]. In fact, a person with a weight of 70 kg contain approximately 3.8 kBq of ^{40}K. In gamma spectrometry the high energy of ^{40}K will result in a Compton continuum spanning over a large portion of the spectrum. Thus, it cause problems as it limits the detection of many gamma ray emitting radionuclides of lower energies than ^{40}K. Activity concentration of ^{40}K in soil is on average 400 Bq/kg around the world[7]. In Sweden this value is even larger, at 780 Bq/kg. Table 1 show average activity concentrations of NORM in the world and Sweden.

Table 1: Average activity concentration of some naturally occurring radionuclides in soil over the world and in Sweden[7].

Region	**^{40}K (Bq/kg)**	**^{226}Ra (Bq/kg)**	**^{232}Th (Bq/kg)**
Sweden	780	42	42
World	400	35	30

Cosmic radiation, in form of protons, electrons and photons contribute to background dose. These particles also interact with the components in the air. This interaction causes oxygen and nitrogen in the air to turn into radioactive nuclides. Specifically there are a few radionuclides originating from cosmic radiation that contributes to the radiation dose of human beings, these are ^{14}C, ^{7}Be, ^{3}H and ^{22}Na also known as cosmogenic nuclides. However these contributions are relatively small compared to the radiation dose emanating from NORM. In high resolution gamma spectrometry, ^{7}Be is noticeable due to its rather large production rate. Cosmic radiation is seen as noise across the entire spectrum in gamma spectrometry. Dose received from cosmic radiation in Sweden is on average 0.3 mSv/year at ground level[6]. Cosmic radiation is reduced by being indoors since materials shield against protons and electrons which cannot penetrate far into materials of increased density. Hence the values above are corrected with the assumption that the population spend 90% of their time indoors. Cosmic radiation received depends on latitude and altitude. Cosmic radiation increase with altitude and with distance from the equator *i.e.* maximum dose is received at the south- and north pole.

2.3 Anthropogenic radionuclides

Anthropogenic radionuclides means that the radionuclides can be derived from human activities. Examples include radionuclides that are produced during operation of a nuclear reactor. Inside a critical nuclear reactor a neutron flux splits heavy nuclei, usually ^{235}U, into smaller ones resulting in release of energy and radioactive fission products and neutrons. Possible fission products are for instance ^{137}Cs, ^{90}Sr, ^{144}Ce and ^{95}Zr. While these are radioactive and should be kept inside the reactor, some fission products are useful for medical purpose or research and can be extracted from the reactor. ^{137}Cs is one of the radionuclides of most concern of the fission products whether the NPP is operating normally, suffer from leakage or in case of a severe accident. Contributing factors to this is that the radionuclide emit gamma rays (662 keV) and has a long half-life (30 y). In addition, it is produced in large amounts along with ^{134}Cs and is effectively absorbed by biomass.

Metallic components and building structures nearby the reactor core may undergo neutron capture when exposed to the reactor neutron flux in which case radionuclides are produced. Examples of neutron activated products are ^{60}Co and ^{54}Mn. ^{60}Co is of particular concern due to its relatively long half-life (5 y) and high-energy gamma rays (1173 keV and 1332 keV).

Around Barsebäck NPP, and as determined in previous surveys of the area, the radioactive contamination is concentrated to two ponds containing sediment consisting of waste sludge. Both ponds contain ^{137}Cs and ^{60}Co and has clear ties to the activities of the NPP. In 1997-98 the bottom of the Barsebäck basin, where the inlet duct of the cooling water is, was dredged and placed on designated land. This created two ponds, the big one called pond A and the small one called pond V. In 2006 the NPPs cooling water outlet duct was cleaned and the sludge was placed in pond V. This further contaminated the pond with ^{137}Cs as well as ^{60}Co. In 2010 it was estimated that the combined activity in the two ponds was 1.9 GBq of ^{137}Cs and 1.1 GBq of ^{60}Co[8]. Thorough measurements of the radioactivity in the ponds was also performed in 2014 and 2021 and displayed elevated levels of ^{60}Co and ^{137}Cs[9, 10]. These resource materials serve as reference values when comparing the results in this report.

2.4 Contamination of anthropogenic radionuclides

When contained inside the reactor, fission and activation products pose no threat to the surroundings due to shielding of the reactor. Small amounts can be released to the environment during normal operation, revision and decommissioning process, but the amounts are strictly controlled and continuously monitored not to exceed the limits set by the regulating authority. Radionuclides may also be discharged to the environment during incidents and accidents. An extreme example of an NPP accident occurred in Chernobyl (1986, Ukrainian SSR), resulting in fission products that spread across the continent of northern Europe leaving the ground radioactive for many years. Anthropogenic radiation contamination can be observed as man-made radioactivity that has spread from one location and then contaminated another location. There are many examples of this but the most prominent ones are the Chernobyl accident and the atmospheric nuclear weapons tests during (mainly) the 1950-1960s, and more recently the Fukushima accident (2011, Japan). Even today traces of these anthropogenic radionuclides from Chernobyl and the nuclear weapon tests can be observed in many parts of Europe. Radionuclides spread with the wind and were deposited onto ground surfaces by either rain or as dry deposition thus contaminating the grounds. In the long term, the radionuclide of most radiological interest is ^{137}Cs due to its relative abundance in the fallout, relatively long half-life and volatility. The nuclear weapon tests released an enormous amount of radioactivity into the atmosphere enabling it to spread globally. Created from the nuclear explosion is a diverse inventory of radionuclides. Fuel materials in a nuclear bomb consist of *e.g.* ^{3}H, uranium isotopes, plutonium isotopes and ^{241}Am. From the explosions, residues of fuel materials are scattered. In addition to this, neutron capture- and fission products created are also spread during the explosion, the most common fission products are presented in Table 2.

Table 2: Some of the most common gamma ray emitting radionuclides originating from nuclear weapon tests[11].

Radionuclide	**Half-life**	**γ-ray energy (keV)**
^{95}Nb	35.0 d	765.8
^{95}Zr	64.0 d	756.7, 724.2
^{131}I	8.0 d	364.5
^{132}I	2.3 h	667.7
^{132}Te	3.2 d	228.3
^{134}Cs	2.1 y	604.7, 795.9
^{137}Cs	30.1 y	661.7
^{140}Ba	12.8 d	537.3
^{140}La	1.7 d	1596.2, 487.0

At the location of Barsebäck NPP, in the region of Skåne, a low radioactive contamination of ^{137}Cs from Chernobyl was found in the ground compared to the much higher levels observed in the northern parts of Sweden[12]. Distribution of ^{137}Cs from Chernobyl was unevenly deposited and at the Barsebäck site the deposition was estimated to 1.17 kBq/m^2 (which is approximately the same contamination levels for the area as from the nuclear weapons tests)[8]. With a half-life of about 30 years the ^{137}Cs activity is now less than half it was in 1986. In pond A and pond V, it is estimated that half of the ^{137}Cs contamination originates from Chernobyl accident and the other half from the Barsebäck NPP operations. The contaminated sediments from dredging the harbour basin and cleaning the outlet duct for cooling water, contained radionuclides from the Chernobyl accident and effluents from the NPP.

2.5 Gamma spectrometry

Gamma spectrometry is a radiation detection method that can, for instance, identify and quantify the occurrence of gamma ray emitting particles in the ground or in a sample. So called *in situ* gamma spectrometry is the use of gamma spectrometry measurement in the environment, stationary in one place, for a set time. The term *ex situ* may be used for measurements of samples that are taken from their original place, for later measurement at another location such as a laboratory. From the measurement it is possible to calculate the activity concentration of certain radionuclides in the ground (Bq/kg) or on the ground (Bq/m^2). A measurement creates an energy spectrum, *i.e.* pulse height distribution, consisting of a distribution of energy depositions in the detector crystal from individual gamma photons. The spectrum contain information about radionuclides present in the measured area (including cosmic component). Figure 2 shows a gamma spectrum obtained from a measurement *in situ* at Barsebäck.

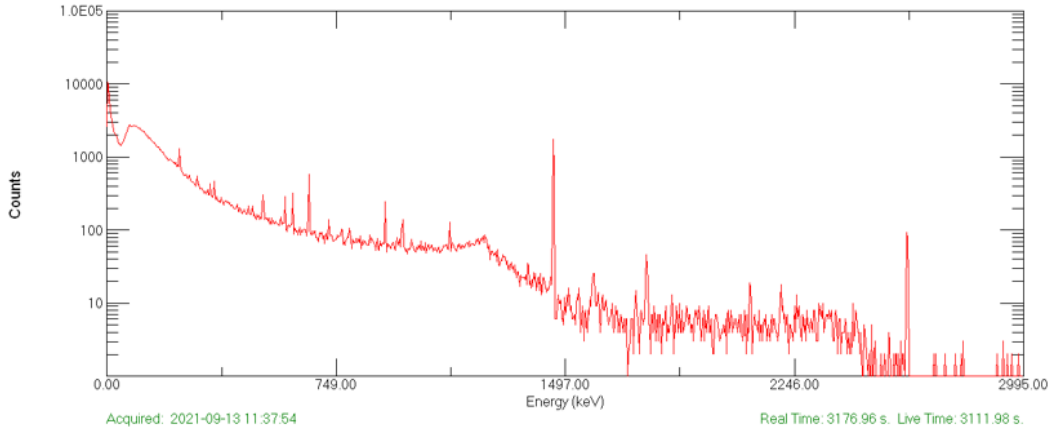

Figure 2: Gamma spectrum from a measurement using a HPGe detector at the Barsebäck NPP area.

The spectrum consist of a histogram where the x-axis show the energy of the gamma rays, converted from channel number in the MCA. On the logarithmic y-axis of the spectrum is the number of counts detected. Examples of detectors that can be used for *in situ* gamma spectrometry are high-purity Germanium (HPGe) semiconductor detectors and Thallium doped Sodium Iodide NaI(Tl) scintillation detectors. HPGe detectors are advantageous to use because of their energy resolution, but with the disadvantages that they are expensive and requires cooling. HPGe detectors can identify and separate gamma radiation from different radionuclides and even resolve peaks of similar energy. In addition, quantification of different radionuclides activity contributions can be determined. NaI(Tl) detectors may also be used for gamma spectrometry. Unlike the HPGe, NaI(Tl) based detectors does not need cooling and are rather inexpensive. However, the energy resolution is not great making it difficult to distinguish peaks of similar energy. NaI(Tl) is sensitive to change in temperature which can create a drift in the energy calibration when used in varying temperatures. An alternative to the HPGe and NaI(Tl) detectors is the Lanthanum(III)Bromide ($LaBr_3$(Ce)) scintillation detector. Compared to NaI(Tl) detectors, it has better energy resolution, but not as good as HPGe detectors[13]. Sensitivity of $LaBr_3$(Ce) detectors in many natural background measurements is lower than NaI(Tl) detectors because they contains small amounts of radioactivity. $LaBr_3$(Ce) has a better temperature stability, meaning the energy calibration is not as sensitive to varying temperatures, and on the other hand it is much more expensive than NaI(Tl) detectors. For field measurements $LaBr_3$(Ce) can be a more optimal option than the NaI(Tl).

Both semiconductor and scintillation detectors must be energy and efficiency calibrated in order to apprehend information from the spectrum. Energy calibration of the detector is done by using a calibration source with a known gamma ray energy such as ^{137}Cs or ^{60}Co. The peak centroid channel correspond to primary gamma energy. The number of peaks needed to energy calibrate a detector depends on the detector type. For *in situ* measurements an energy calibration based on at least two full energy peaks is generally sufficient to produce a meaningful linear energy response. In a scintillation detector, 4-5 peaks are used for energy calibration. Both detector types do, however, require the detectors efficiency of known

energy across the whole spectrum for a given geometry to achieve a reliable efficiency calibration. For gamma spectrometry in laboratory studies, it is also necessary to do this for different densities and geometries of the samples. Since the energy calibration of a gamma spectrometry detector may change when moving it between two places, this needs to be corrected for when *in situ*. ^{40}K is present in the environment and its peak will be clearly visible in any spectrum almost anywhere in Sweden. Its gamma-ray energy is known and thus it can be used to perform an energy calibration. During radioactive fallout or in other countries there can be dominant peaks of something else depending of the radiological environment. If the contamination consists of ^{137}Cs (or the dominating radionuclides are known) it can be used as a substitute for ^{40}K or a calibration source might be necessary.

2.6 Activity calculation

Full absorption of a gamma photon results in a peak in the spectrum. Peaks net area represent the total number of events for a certain energy of the gamma radiation. Radionuclides can be distinguished and identified through analysis of the spectrum, either automatically using a software or manually using radionuclide data tables and the detector calibration. A radionuclide of interest is presented as a peak and its activity can be calculated using the following method explained below[14]. Peak area is obtained by selecting a region of interest (ROI) over a specific peak. This will generate the total number of counts in that peak. The peak also consist of a continuum of counts from *i.e.* Compton scattering and noise that has to be subtracted from the total counts in the ROI. Hence the equation

$$N_{Peak} = N_{Total} - N_{Background}, \tag{2.1}$$

where N_{Peak} calculates the net number of counts in the peak and N_{Total} is the total number of counts in the ROI. $N_{Background}$ is the number of counts from the continuum. Assuming a linear continuum, the number of background counts in the ROI can be calculated using

$$N_{Background} = \left(\frac{Ch_{Peak}}{2Ch_{Side}}\right)(B_1 + B_2), \tag{2.2}$$

where Ch_{Peak} is the number of channels in the ROI, Ch_{Side} is the number of channels chosen on each side of the ROI. B_1 and B_2 are the total number of counts in the chosen side channels on respective side.

Counts provided through measurements are associated with errors and uncertainties. Statistical uncertainty arise due to fluctuations in the Poisson distribution. An effort to account for these uncertainties is to apply uncertainty calculations. The uncertainty of the peak can be calculated with uncertainty propagation using the uncertainty of both the total number of counts as well as the uncertainty of the counts in the continuum. Standard deviation (σ_{Total}) is the total number of counts calculated by taking the square root of the number of counts, according to Poisson statistics[15].

$$\sigma_{Total} = \sqrt{N_{Total}}. \tag{2.3}$$

Where multiple uncertainties are present such as uncertainty calculations of peaks, uncertainty propagation must be used. Uncertainty propagation is calculated by involving both the total number of counts and the background counts of the continuum. Hence the uncertainty of the number of counts in the peak is determined by the equation

$$\sigma_{Peak} = \sqrt{\sigma^2_{Total} + \sigma^2_{Background}}, \tag{2.4}$$

where the indices note where the uncertainty is in the number of counts. The uncertainty of background counts is not as straight forward as for the uncertainty of total counts and hence, uncertainty propagation must be used which lead to

$$\sigma_{Background} = \sqrt{\left(\frac{Ch_{Peak}}{2Ch_{Side}}\right)^2 \sigma^2_{B1} + \left(\frac{Ch_{Peak}}{2Ch_{Side}}\right)^2 \sigma^2_{B2}}, \tag{2.5}$$

where σ_{B1} and σ_{B1} are the standard deviation of number of counts of each side of the ROI.

A peak in a spectrum implies that there is a radionuclide present emitting gamma radiation of certain energy, however, this is not always true. Peak analysis in a spectrum involves determination if the radionuclide is present or not. Thus, the concept of a detection limit (L_D) is to determine if a signal (a characteristic peak of a radionuclide) is indeed present in the measurement. Detection limit is defined based on the degree of confidence placed on certainty of detection. In Figure 3 a peak is represented using a 95% and 99.7% confidence interval in counts, corresponding to 2σ and 3σ, respectively. Where the black lines represent a 95% confidence interval and the red line represent a 99.7% confidence interval.

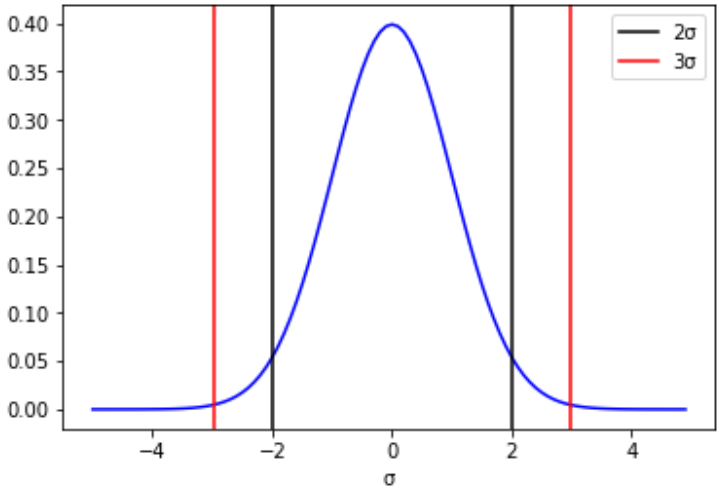

Figure 3: Gaussian function displaying the confidence level of 95% (black line) and 99.7% (red line)[14].

These are the most common confidence levels used for hypothesis testing. According to the definition by Currie[16], detection limit with a confidence level of 95% is defined as

$$L_D = 2.71 + 4.65\sigma_{Background}, \tag{2.6}$$

where it is clearly shown that the detection limit is proportional to the uncertainty in the background counts. It is used for calculations of a threshold value of activity

which provide a minimum detectable activity (MDA). MDA is calculated using the equation

$$MDA = \frac{L_D}{\epsilon \cdot n_\gamma \cdot t_{live}}, \tag{2.7}$$

where ϵ is the detector efficiency at the gamma energy of the measured radionuclide, n_γ is the branching ratio of emission of the specific isotopes gamma radiation and t_{live} is the live time of the detector measurement.

Calculation of activity is similar to that of MDA with a few additions. Note that the efficiency is energy dependent. Thus, efficiency is specific for each gamma energy.

$$A = \frac{N_{Peak} \cdot k_D \cdot k_{tcs}}{\epsilon \cdot n_\gamma \cdot t_{live}}, \tag{2.8}$$

k_D and k_{tcs} are correction factors for decay and true coincidence summation respectively. Decay correction is calculated with

$$k_D = e^{-\lambda t}, \tag{2.9}$$

where λ is the decay constant and t is the time between the measurement and time of sampling (or other event). Uncertainty in activity is calculated using the uncertainty propagation method since only two factors are considered here that contributes to the uncertainty. These two factors are the uncertainty in counts and uncertainty in detector efficiency (σ_ϵ). Hence, uncertainty in activity (σ_A) is calculated using the equation

$$\sigma_A = \sqrt{\sigma^2_{N_{Peak}} \left(\frac{k_D \cdot k_{tcs}}{\epsilon \cdot n_\gamma \cdot t_{live}} \right)^2 + \sigma^2_\epsilon \left(\frac{N \cdot k_D \cdot k_{tcs}}{\epsilon^2 \cdot n_\gamma \cdot t_{live}} \right)^2}. \tag{2.10}$$

2.7 Ambient dose equivalent rate

Ambient dose equivalent rate (ADER) is used as an operational quantity in radiation protection for area monitoring, and is linked to the personal dose equivalent ($H_p(10)$) for individual monitoring. ADER is denoted by $\dot{H}^*(10)$ and uses the unit Sv/h. By definition it is the dose equivalent, from radiation incident orthogonal to a spheres surface, to a point at 10 mm depth in a sphere (30 cm diameter) composed of tissue-like material, per time unit[17]. An organic scintillator probe (6150AD-b/E, Automess, Germany) can perform field measurement of this quantity. Utilization of ADER gives an indication of the external dose in an area. Dose limits are set by the regulating authority of each country but in most European countries it follows the recommendations given in the European directive on radiation protection (Directive 2013/59/Euratom). In Sweden, SSM is responsible for setting dose limits and they follow the above mentioned Euroatom directive. Dose limits concern occupational radiation exposures as well as exposures of the general public (but not for medical diagnostics or therapies). A limit for exposure of the general public exist so that deterministic effects are prevented and to minimize the stochastic effects radiation may induce. In general, the linear non-threshold model is used to assess the risk of radiation induced cancer. The model states that there is no threshold to radiation induced health detriments, even small radiation doses contribute to the

risk. For the general public, an effective dose limit is set to 1 mSv/year as for the total exposure from all activities that generate radiation[18, 19]. This include the condition of 0.1 mSv/year originating from a single activity. Hence when assessing the ground at the Barsebäck site the latter will be the clearance level to compare to the result since contamination from past activities and decommissioning of the NPP counts as one instance towards dose assessment. However, there will always be a large contribution of background radiation and thus, in order to account for this the background must subtracted from the total ADER. Average external dose provided from natural background *i.e.* NORM and cosmic radiation is on average 0.9 mSv/year in Sweden with regional and individual variations[6].

2.8 Dose rate calculations with a spectrometer-dosimeter

A spectrometer-dosimeter, AT6101D (ATOMTEX, Belarus), is a multi-purpose radiation detection tool based on a NaI(Tl) detector. In addition to gamma spectrometry, it can measure ADER with the ability to distinguish the effective activity concentration of NORM radionuclides. By doing dose rate measurements it is possible to calculate the dose rate contribution from anthropogenic radionuclides according to a model presented by Valerey Ramzaev *et al*.[20]. As this unit is portable, it can be used in a laboratory environment as well as outdoors for *in situ* measurements and backpack measurements. The material and methods section contain a more in-depth description of the AT6101D. In order to get the total ADER, no calculations are needed, it is sufficient to use a handheld radiation protection instrument. However, using the AT6101D for such measurements add additional information about the effective activity concentration of NORM radionuclides. With calculations it is possible to separate the ADER components presented in the following equation

$$ADER_{total} = ADER_{NORM} + ADER_{cosmic} + ADER_{int} + ADER_{ant}, \tag{2.11}$$

where ADER_{NORM} is the contribution from terrestrial radionuclides, ADER_{cosmic} is the contribution from cosmic radiation, ADER_{int} is the contribution from intrinsic noise in the detector. ADER_{ant} is the contribution from anthropogenic radionuclides present *e.g.* ^{137}Cs and ^{60}Co. ADER from cosmic radiation and intrinsic noise can be measured by choosing measuring site carefully where no other radionuclides contribute to the dose. One way to determine ADER_{NORM} is by doing measurements of the cosmic radiation and intrinsic noise along with a background measurement where the contribution from anthropogenic radionuclides are negligible. Following this criteria the equation simplifies to

$$ADER_{NORM} = ADER_{total} - ADER_{cosmic} - ADER_{int}. \tag{2.12}$$

ADER_{NORM} can also be calculated using the effective activity concentration (AC_{eff}) from ^{40}K, ^{226}Ra and ^{232}Th with a conversion factor (CC) according to equation 2.13.

$$ADER_{NORM} = AC_{eff} \cdot CC. \tag{2.13}$$

The effective activity concentration, AC_{eff} (Bq/kg), is closely related to radium equivalent activity whose factor describe how much activity concentration of a radionuclide is equivalent to the gamma dose rate generated by ^{226}Ra. In the case of the terrestrial radionuclides the equation becomes

$$AC_{eff} = AC_{^{226}Ra} + 1.31 \cdot AC_{^{232}Th} + 0.085 \cdot AC_{^{40}K}. \tag{2.14}$$

The coefficients are set values programmed into the AT6101D detector, enabling it to perform calculations of the terrestrial effective activity concentration. The conversion factor is obtained by regression analysis of effective activity concentration and total ADER from multiple background measurement[20]. Determination of ADER_{NORM} allows for calculation of ADER_{ant}, by using equation 2.11 to isolate ADER_{ant} to one side of the equal sign.

Chapter 3

Material and methods

The general work structure was to identify locations for performing measurements and collect soil samples in the area of Barsebäck NPP, both inside and outside the fenced area. Providing additional coverage of the locations from mobile measurements. All the measurements and soil samples would then be prepared and analysed in parallel for radioactive contamination and NORM in the laboratory. The results of the analysis would then be validated and interpreted.

3.1 Preparations

Extensive planning beforehand is essential for the study to be successful and time efficient as there are many parameters to consider. One such thing is what kind of measurements are suitable for answering the research question. The choice of measurement method can be decided depending on already existing information of the area and from radiological characterization efforts made in the past. The measurement sites can be determined probabilistic as a strategy of choosing sites. But usually it is well known within the NPP sites where the probability of finding radioactive contamination is high and thus these locations are chosen as primary measurement sites. However, if the radiation levels are not known beforehand, it is possible to do a mobile survey of the area (by *e.g.* foot, car or drone) in order to identify areas with elevated radioactivity levels. To efficiently cover the ground with measurements there are a number of different methods available. Methods of choice for this thesis included

1. *In situ* gamma spectrometry with HPGe- and NaI(Tl)-detectors.
2. Soil samples analysed with lead-shielded HPGe detectors in laboratory.
3. Mobile gamma spectrometry with $LaBr_3$ detector.
4. Dose rate measurements with scintillator probe.

3.2 Radiological characterization of areas at Barsebäck NPP

A large number of measurements are needed to do a thorough assessment of the radiation environment. It may include measurements in grass, crops, water, sludge, different water bodies and foodstuff in the nearby area. However, it was not possible to include all of these measurements in the scope of this report as it would be too time and resource consuming. Instead, a reasonable amount of measurements in the area was made with *in situ* as well as mobile gamma spectrometry and soil

sampling. These measurements grant an insight in what the radiological environment looks like, without including transfer pathways to human internal dose. In addition to this, the ambient dose equivalent rate was obtained for the different locations. Many of the measurements were carried out simultaneously in order to be as time efficient as possible. Thus, it was possible to acquire as much data as possible within the given time frame. Figure 4 show the 10 sites chosen for *in situ* measurements around Barsebäck NPP. Also, it should be noted that potential contamination of the area due to discharges of alpha emitting nuclides such as ^{238}Pu and transuraniums were not considered in this work. Figure 4 show measurement sites outside and inside the fenced area and in Table 3 each site is described. It was unclear whether the soil in many of the sites were disturbed after 1986 or not.

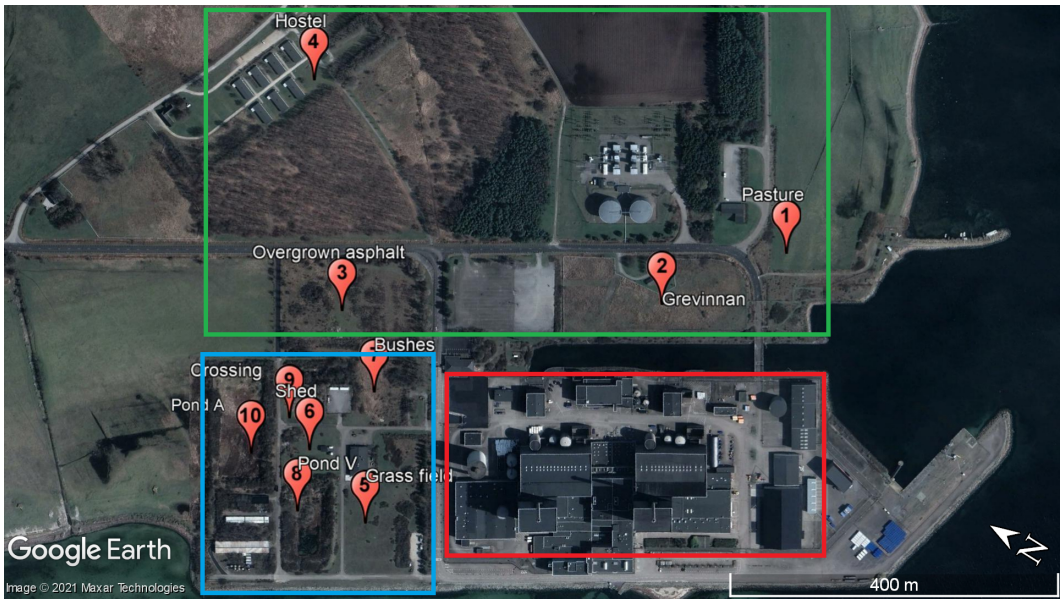

Figure 4: Map of sites 1-10 where *in situ* measurements were performed. The blue and red rectangles constitute the fenced industrial zone where parts of the red area is defined as restricted area. Measurements in the red area consisted of mobile gamma spectrometry by backpack. The area indicated in green rectangle is outside the NPP site.

Table 3: Site description of the measurement locations in the Barsebäck NPP area.

Site	Name	Description	Coordinates
1	Pasture	Soil, grass- and rocky-terrain	55°44'37.9"N, 12°55'36.6"E
2	Grevinnan	Soil, high grass	55°44'40.6"N, 12°55'28.7"E
3	Overgrown asphalt	Asphalt, grass and plants	55°44'51.6"N, 12°55'16.7"E
4	Hostel	Soil, nearby living quarters	55°44'56.9"N, 12°55'29.0"E
5	Field south of pond V	Soil, grass and bushes	55°44'46.2"N, 12°55'04.4"E
6	Old fire station	Soil, grass and bushes	55°44'49.3"N, 12°55'07.2"E
7	Bushes	Soil, high grass and bushes	55°44'48.5"N, 12°55'12.5"E
8	Pond V	Soil, rocks, bushes, grass and water	55°44'48.8"N, 12°55'02.6"E
9	Crossing	Soil, grass and bushes	55°44'50.8"N, 12°55'08.6"E
10	Pond A	Soil, mud, water, reeds	55°44'51.5"N, 12°55'04.3"E

3.3 Gamma spectrometry

3.3.1 Assessments using a HPGe detector

For *in situ* gamma spectrometry at the selected sites in Table 3 and Figure 4, a Canberra GC2018 S/N:b16067 high purity germanium semiconductor detector was used. It is a p-type HPGe detector, with a relative efficiency of 20%. The HPGe detector was placed on a tripod so that the detector was directed downward towards the ground at a height of 1 meter above ground. It was necessary to place the setup in an open area on a flat surface without interfering objects in the field of view of the radiation. The detector was connected to a digital multi-channel-analyzer (MCA) (Digidart, USA). High voltage (2500V) was applied with the MCA, so that the detector was able to collect data during the measurement. The duration of data acquisition varied between the sites but the measurement duration lasted at least 45 minutes where the longest measurement was 123 minutes and the average was 78 minutes for all sites. After each measurement, the spectral data was saved to the MCA for later processing in the laboratory.

Figure 5: *In situ* gamma spectrometry at site 1 with a HPGe detector.

Energy configurations were performed before the measurement started to acquire spectrum data from the HPGe detector. This included selecting 2048 channels for representing the energy interval and setting the gain, so the centroid channel of the ^{40}K peak was centered in channel 1000. During analysis after the measurement, radionuclides of interest were marked in the spectrum, each with a ROI and the background corrected counts was displayed. Selection of these radionuclides was based on expected contamination as well as NORM contributions. Hence, anthropogenic radionuclides of ^{60}Co and ^{137}Cs were of special interest. For calculations of these anthropogenic radionuclides a thin slab geometry was used. This assumes that the anthropogenic contamination is fresh and only penetrate roughly

2.5 cm into the soil. Radionuclides from NORM are many and thus, only one easily detected radionuclide was selected from each decay chain. There were many radionuclides to choose from and in the end the choice was made to include ^{226}Ra from the uranium series and ^{228}Ac from the thorium series. ^{235}U, that would be chosen as a representative radionuclide of the actinium series emit a low energy gamma ray which is difficult to differentiate from the background. In addition, the contribution from the actinium series is very low compared to uranium- and thorium series. Thus, ^{235}U was neglected in this report. ^{40}K was included since it contributes significantly to the background radiation from the ground. Because the NORM radionuclides was assumed to be uniformly distributed in the soil of the ground, a detector efficiency based on homogeneous distribution in the soil was applied for calculations. ^{7}Be is produced in the atmosphere and was selected because of its contribution to the background radiation. Using equation 2.8 the activity concentration or surface activity, depending on which efficiency calibration used, was calculated along with corresponding uncertainty using equation 2.10. Relevant data such as branching ratio and half-life of radionuclides were collected from Laraweb[21]. Activity concentration was calculated for ^{40}K, ^{226}Ra and ^{228}Ac while surface activity was calculated for ^{137}Cs, ^{60}Co and ^{7}Be at all sites. ^{226}Ra was calculated using ^{214}Bi by assuming secular equilibrium in the uranium series. The result was compared to similar measurements carried out in recent years in a nearby area in Lund, around the European Spallation Source (ESS)[22]. Decay correction was used on the theoretical contamination from 1986 of 1.2 kBq/m^2 to compare with the *in situ* HPGe measurements. Subtracting this value from the experimental value yield a result, where positive values are an indication of further contamination in addition to contamination from the Chernobyl accident and the nuclear weapon tests.

3.3.2 Assessments using a spectrometer-dosimeter

The spectrometer-dosemeter, AT6101D, is equipped with a 63(ø) mm$\times$63 mm NaI(Tl) scintillation crystal enabling gamma spectrometry with a maximum detection efficiency of 8% for ^{137}Cs (662 keV) as a surface source (Bq/m^2). The uniqueness, compared to a regular scintillator detector, is the ability to separate contributions from NORM radionuclides ^{40}K, ^{226}Ra and ^{232}Th to the total dose rate. By utilizing this, the detector can distinguish the ADER from NORM radionuclides, resulting in a dose estimate from anthropogenic radionuclides such as ^{137}Cs[20]. Furthermore, this allows for comparing ADER at each site against the existing dose limit for the anthropogenic dose contribution.

As the detector was brand new, the center of the scintillation crystal was located and marked on the casing, by acquiring an X-ray image of the detector. Measurements were then performed in the same systematic process at all sites, positioning the crystal at a height of 1 m and/or 0.1 m above the ground surfaces.

The goal of the measurements was to measure the combined activity concentration of the NORM radionuclides (AC_{eff}), and the total dose rate of all radionuclides present at each site ($ADER_{total}$). With knowledge of these two parameters, a conversion coefficient (CC) can be obtained through regression analysis. The conversion coefficient is then used to convert AC_{eff} to $ADER_{NORM}$. Before starting measurements the detection unit (DU, (orange in Figure 6)) had to be calibrated. This process is semi-automated by connecting the information processing unit (IPU) to

the detector unit and entering stabilization mode. A calibration source containing potassium chloride (KCl) was positioned in front of the detector crystal and the energy vs channel calibration starts automatically to position the full energy peak from ^{40}K at the correct position in the spectrum. When the DU was calibrated, it was placed on the site using a tripod. Minimum duration of the measurement was set to 15 minutes with an average measurement time of 18 minutes and 21 minutes for the 1 m and 0.1 m heights, respectively.

Figure 6: AT6101D *in situ* gamma spectrometry/ADER measurement 0.1 meter and 1 meter above ground at site 9.

To improve calculations of the conversion coefficient, a series of background measurements were carried out. From the measurements made with the HPGe detector it was possible to conclude that some of the sites could be used as background measurement sites. These sites had a low ^{137}Cs surface activity (<200 Bq/m^2). Graphs were plotted for the background data obtained at 0.1 meter and 1 meter with AC_{eff} on the x-axis and the corrected background ADER on the y-axis. The spectrometer-dosimeter automatically calculated AC_{eff} by using equation 2.14. Through regression analysis of the values, a conversion coefficient in nSv/h per Bq/kg was obtained. Using equation 2.13 the effective activity concentration of the terrestrial radionuclides was converted into $ADER_{NORM}$.

For calculations of $ADER_{ant}$ in equation 2.11, an additional measurement was performed. The measurement took place 240 m out on a long wooden pier in the ocean (approximate depth 1.5 m and 2 m above the ocean) and the duration was 22 minutes. Measurement at this location (see Figure 7) yield a very low amount of gamma rays from terrestrial radionuclides *i.e.* $ADER_{NORM}$. A measurement was also carried out on the beach where NORM contribution to background radiation is generally low.

Figure 7: Measurement of the cosmic radiation and intrinsic noise of the detector components on the pier.

The intrinsic noise of the detector ($ADER_{int}$) was measured for 30 minutes inside an iron shielded room (normally used for whole body measurements of radionuclide concentration) at a temperature of ∼20°C. Background radiation, such as cosmic radiation, is minimized due to the shielding properties of the iron.

Figure 8: Measurement of the ADER intrinsic noise component within the detector in an iron shielded room.

$ADER_{ant}$ was calculated by subtracting the ADER contributions from the sum of cosmic radiation, intrinsic noise from the detector and $ADER_{NORM}$, from the total ADER in equation 2.11.

3.3.3 Soil samples

Collection of soil samples was performed at all sites where *in situ* gamma spectrometry was carried out, except at sites 3, 8 and 10. Site 3 consisted of a hard surface, probably asphalt or gravel below the vegetation. At site 8, representing the area around pond V, the ground consisted solely of rocks making it impossible to collect soil samples. The rock filled surface is probably due to the creation of the pond when sediment from the NPP harbour and cooling water outlet was

relocated there. At site 10, representing pond A, no soil samples were gathered either due to the pond being partly covered by water in addition to being overgrown by reeds. It was however possible to carefully walk across the pond because of the reeds that laid as a cover over the water and mud.

The soil sampling strategy was selected to represent an almost identical sampling pattern at all measurement sites, with a time efficient number of samples to ensure a sufficient representation of the radionuclide inventory at each site. In order to maintain identical soil sampling at each site, a rope of a specific length was placed in a square with the HPGe detector in the center. A total of five soil samples were collected at each site, where one sample was taken from each corner of the square and one sample at the center. Each such sample consisted of a soil core with a length of 20 cm and a diameter of 5 cm. A sledge hammer was used to press the sampler deep enough into the ground. Each of the five 20 cm samples was then divided into 5 layers: surface, 0-5 cm, 5-10 cm, 10-15 cm and 15-20 cm. The fractions of soil from each layer were placed in individual plastic bags and marked with ID, date and depth of the layer. For some locations it was not possible to collect soil samples below 10 cm because of rocks. This included all sites located inside the fenced area of the NPP. The reason being the ground was constructed artificially before the NPP was built. At sites 1-4, samples at a depth of 20 cm was collected and at sites 5-10, excluding 8 and 10, samples at a depth of 10 cm was collected.

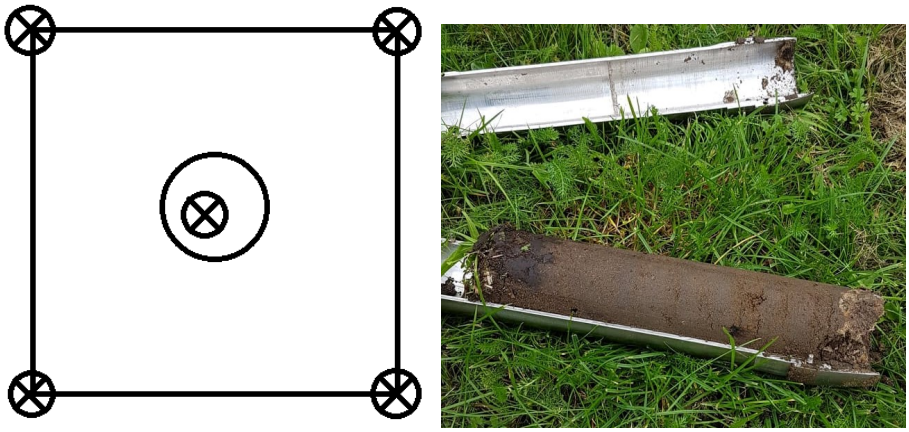

Figure 9: To the left: soil sampling strategy at each location (circles with cross) and the HPGe (big circle) placed in the center. To the right: picture of a 20 cm soil core collected at site 4.

The soil was dried in the laboratory, at Medical Radiation Physics in Malmö, by distributing the samples on paper sheets and measuring their individual weights. The sheets with soil were then put in a heating cabinet to remove all water content from the sample. The temperature was set to 70°C for 95 minute cycles. Between the cycles the samples were mixed for making the drying process faster and homogeneous. When the water was removed the weight of the dried samples were registered. The soil samples were put in either 60 ml or 200 ml plastic beakers, depending on the amount of soil available. Small variations in sample weight in the beakers are due to variations in soil compositions, rather than the filling amount.

The dried soil samples were analysed by gamma spectrometry, with the above

mentioned geometries, using three different lead-shielded HPGe detectors for identification of gamma ray emitting radionuclides. The relative efficiency of the detectors named 4, 5 and 7 was 55%, 92.5% and 100%, respectively. Each measurement resulted in a spectrum that was analysed with GammaVision (ORTEC, USA). For these measurements the efficiency calibrations were performed using geometries prepared from a certified reference multinuclide solution traceable to NIST. Evaluation of the spectrum data enabled calculations of the activity concentration (Bq/kg) using a standardized excel sheet. The laboratory participate in IAEA (International atomic energy agency) annual proficiency test. Corrections were made for decay as well as true coincidence summing. Included in the excel sheet was the calculation of MDA for all radionuclides using Curries method[16]. The duration of the gamma spectrometry was >48 h, for each sample, in order to get reasonable counting statistics in the spectrum. Reference date of each sample was the date the sample was obtained from each location. After the measurement the samples were stored accordingly.

3.3.4 Mobile gamma spectrometry

In contrast to *in situ* gamma spectrometry, a specially designed backpack detector system was used to make mobile spectrometry and measurements of the dose rate 1 meter above the ground. With this method it was possible to check for variability in dose rate at each site and other areas not covered by *in situ* measurements or soil sampling. The system consisted of a pc laptop connected to a 3.8(ø) mm$\times$3.8 mm $LaBr_3$(Ce) scintillation detector coupled to a DigiBase (ORTEC, USA) photo multiplier tube (PM-tube) base which was held in a backpack together with electronics and a GPS. The detector was configured and started by Maestro (ORTEC, USA), a software for spectrum analysis that allowed to calibrate the energy by doing a background measurement. The energy interval was chosen to be represented by 1024 channels on the analog to digital converter (ADC). In the environment around Barsebäck, ^{40}K contributes the most to the radiation background and its peak was used to define the energy channel 500 by setting the gain of the detector in Maestro. Once the gain was set, the software Nugget was used, which was developed at SSM[23]. Nugget is generally used for emergency preparedness applications. Current dose rate in Nugget utilizes spectrum dose index (SDI) presenting the total photon dose rate[24, 25]. An energy dependent factor, which was automatically chosen by the software, was multiplied with the number of detected pulses in a pulse height distribution. It then becomes known as SDI-dose rate. Nugget then link the SDI-dose rate and the GPS signal to generate a map of the measurements. Each measurement was started after putting on the backpack and then walking to a corner in the area of interest, followed by walking in a line along the edge to the adjacent corner. Moving in parallel lines spread by approximately 1.5 m inside the area of interest until the whole area had been covered. Backpack measurements generated full coverage of the dose rate and spectrum information at the areas around each site, both inside and outside, of Barsebäck NPP site.

Mobile gamma spectrometry measurements using backpack equipment were performed at all sites including additional coverage of the area inside the fence. These were given an ID instead of a site number. Site numbers range from 1-10 while ID range from 11-19. In addition, mobile gamma spectrometry measurements were done using a car-borne measurement system. This enabled faster and

more efficient coverage of roads in the area of the NPP. Dose rate for car-borne measurement was displayed in SDI-dose rate just like the backpack measurements. The specially equipped car had 2×4 *l* NaI(Tl)-detectors installed. The car was moving with a low speed (20-30 km/h) where at the same time spectra was recorded, using an integration time of 1 s of the NaI(Tl) detectors.

Converting SDI-dose rate to ADER was performed by cross calibrating with the average ADER at each site which was obtained from the scintillation probe measurements. For those locations that were not connected to a specific site number, ADER was estimated based on assessment of the local terrain. Data gathered from mobile gamma spectrometry measurements was processed using Python and Earth Point tool to obtain a file that could be uploaded to Google Earth where the dose rate was mapped for the coordinates that were registered[26]. Figure 10 show the restricted area (marked red in Figure 4) where five sections were measured with mobile gamma spectrometry. Each sections was given a corresponding ID for the respective backpack measurements.

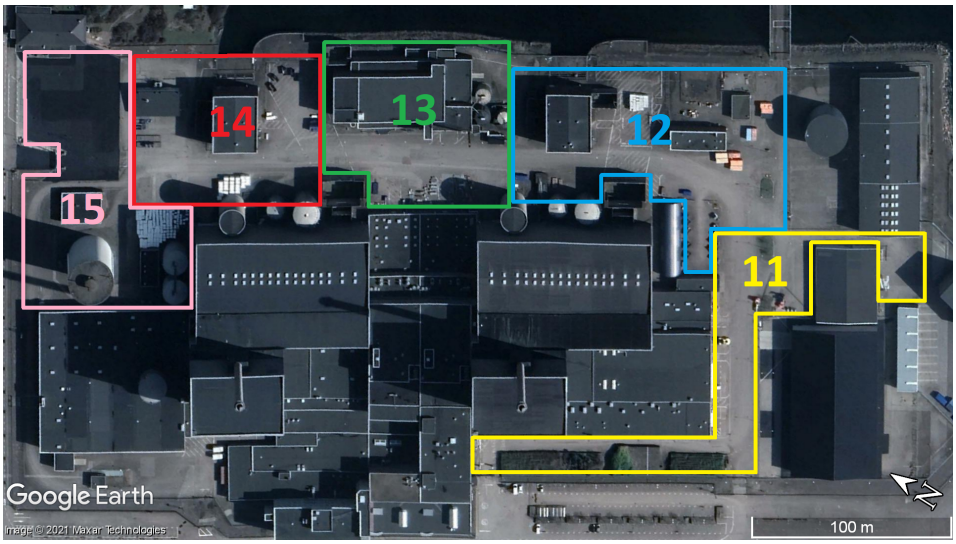

Figure 10: Restricted area coverage with mobile gamma spectrometry using backpack.

3.4 Ambient dose equivalent rate

The ambient dose equivalent rate was determined using two methods: the AT6101D, which has the ability to measure ADER for radiological risk assessment with good accuracy. ADER measurements and gamma spectrometry measurements were carried out simultaneously at all 10 sites with this detector, plus an additional location close to site 8, converting site 8 into 8.1 (old site 8) and 8.2 (new location). The other instrument was Automess hand-held radiation protection detector (model 6150) coupled with a scintillation probe. The scintillation probe was positioned 1 m above ground on a tripod at four to five different positions in each site. It was placed several meters away from the *in situ* gamma spectrometry position pointing towards the HPGe. Measuring for at least 15 minutes at each position, an average ADER for each site was obtained. For each site, ADER was calculated in terms of maximum, minimum, average and standard deviation.

Figure 11: Handheld radiation protection unit (left) and scintillator probe on a tripod facing the HPGe detector(right).

Chapter 4

Results

4.1 Gamma spectrometry

4.1.1 Assessments using a HPGe detector

Activity concentration of NORM and anthropogenic radionuclides from *in situ* gamma spectrometry are presented in Table 4 and 5 along with one standard deviation. Table 4 and 5 also show the average activity concentration of NORM and anthropogenic radionuclides respectively, inside and outside the fence.

Table 4: NORM activity concentration from *in situ* gamma spectrometry measurements presented with uncertainty of one standard deviation for values above MDA. Activity concentration and MDA is presented in Bq/kg except for ^{7}Be where it is presented in Bq/m^2.

	^{226}Ra		^{40}K		^{228}Ac		^{7}Be	
Site	**A**	**MDA**	**A**	**MDA**	**A**	**MDA**	**A**	**MDA**
1	10 ± 1	1	655 ± 16	6	14 ± 2	2	404 ± 110	243
2	13 ± 2	1	400 ± 14	4	12 ± 1	2	301 ± 128	204
3	15 ± 2	1	394 ± 14	4	12 ± 2	2	368 ± 142	224
4	10 ± 1	1	319 ± 10	3	11 ± 1	1	208 ± 82	131
5	26 ± 1	1	522 ± 17	5	20 ± 2	2	560 ± 181	155
6	20 ± 1	1	408 ± 14	4	16 ± 2	2	341 ± 159	196
7	18 ± 1	1	333 ± 11	3	13 ± 1	2	216 ± 71	158
8	18 ± 2	2	450 ± 15	4	17 ± 1	2	357 ± 113	181
9	23 ± 1	2	403 ± 15	5	20 ± 2	2	306 ± 159	257
10	11 ± 1	1	197 ± 9	5	10 ± 1	2	536 ± 132	207
Location	**Avg. ^{226}Ra**		**Avg. ^{40}K**		**Avg. ^{228}Ac**		**Avg. ^{7}Be**	
Outside fence	12		442		12		320	
Inside fence	19		386		16		386	
All sites	14		414		15		353	

Table 5: Activity concentration of some anthropogenic radionuclides of special interest from *in situ* gamma spectrometry measurements presented with uncertainty of one standard deviation for values above MDA. Activity concentration and MDA is presented in Bq/m^2.

	^{137}**Cs**		^{60}**Co**	
Site	**A**	**MDA**	**A**	**MDA**
1	407±17	29	<MDA	37
2	187±15	17	35±10	17
3	39±14	19	<MDA	18
4	161±10	11	<MDA	11
5	99±19	19	28±10	19
6	153±17	16	9±16	8
7	397±13	18	20±9	12
8	68±12	22	65±14	22
9	569±22	38	67±12	20
10	719±21	25	79±13	22
Location	**Avg. ^{137}Cs**		**Avg. ^{60}Co**	
Outside fence	199		35	
Inside fence	334		58	
All sites	267		47	

Decay correction of the theoretical contamination of anthropogenic radionuclides from the Chernobyl accident and nuclear weapon tests at Barsebäck NPP site was calculated to 0.52 kBq/m^2.

In situ gamma spectrometry measurements results from AT1601D show the activity concentration of NORM radionuclides in Table 6 and 7, at 0.1 meter and 1 meter distance, respectively. The effective activity concentration of NORM radionuclides is also provided in these tables.

Table 6: NORM activity concentration measured with *in situ* gamma spectrometry at 0.1 meter presented with uncertainty of one standard deviation. All activity concentrations are shown in Bq/kg.

Site	**Time (s)**	^{226}**Ra**	^{40}**K**	^{228}**Th**	**AC**$_{eff}$
1	1117	13 ± 4	617 ± 123	13 ± 3	82 ± 10
2	1029	9 ± 4	646 ± 129	22 ± 5	92 ± 11
3	1010	14 ± 5	528 ± 106	18 ± 4	83 ± 9
4	1226	15 ± 4	472 ± 94	14 ± 4	74 ± 8
5	2002	18 ± 5	940 ± 188	31 ± 7	138 ± 13
6	1142	15 ± 5	481 ± 96	16 ± 4	77 ± 8
7	1376	18 ± 5	540 ± 108	17 ± 4	87 ± 9
8.1	1465	23 ± 6	1030 ± 210	41 ± 9	163 ± 15
8.2	915	7 ± 4	722 ± 144	26 ± 5	101 ± 12
9	1005	17 ± 5	578 ± 116	22 ± 5	94 ± 10
10	1267	11 ± 4	276 ± 58	15 ± 4	55 ± 6

Table 7: NORM activity concentration measured with *in situ* gamma spectrometry at 1 meter presented with uncertainty of one standard deviation. All activity concentrations are presented in Bq/kg.

Site	Time (s)	^{226}Ra	^{40}K	^{228}Th	AC_{eff}
1	949	6 ± 3	613 ± 123	17 ± 4	80 ± 10
2	935	11 ± 5	639 ± 128	23 ± 6	95 ± 11
3	990	10 ± 4	551 ± 110	20 ± 5	82 ± 9
4	942	5 ± 3	450 ± 91	17 ± 4	65 ± 8
5	1661	9 ± 4	827 ± 165	31 ± 7	117 ± 12
6	1041	8 ± 4	619 ± 124	24 ± 6	90 ± 10
7	1032	7 ± 4	541 ± 108	20 ± 5	78 ± 9
8.1	1089	15 ± 5	701 ± 140	27 ± 6	109 ± 11
8.2	947	7 ± 4	633 ± 127	23 ± 5	89 ± 11
9	1041	16 ± 5	643 ± 129	30 ± 7	109 ± 11
10	1192	7 ± 3	301 ± 63	16 ± 4	53 ± 6

4.1.2 Assessments using a spectrometer-dosimeter

Background measurements with the AT1601D spectrometer-dosimeter performed at the pier gave an ADER value of 5 nSv/h. On the beach the ADER value was 30 nSv/h. Corresponding ADER measurements in these locations with the scintillator probe were 64 nSv/h and 30 nSv/h, on the beach and the pier respectively. The intrinsic noise of the detector was 3 nSv/h obtained from the measurement in the iron shielded room. The conversion coefficient (CC), presented in Figure 12, was calculated using n=14 measurements, 7 of which were carried out at 1 meter and the other 7 at 0.1 meter from the ground. Regression analysis gave a CC of 0.5 (nSv/h)/(Bq/kg). The intercept of the regression line was calculated to 10 nSv/h. This can be interpreted as the contribution from intrinsic noise of the detector, cosmic radiation and cosmogenic radionuclides.

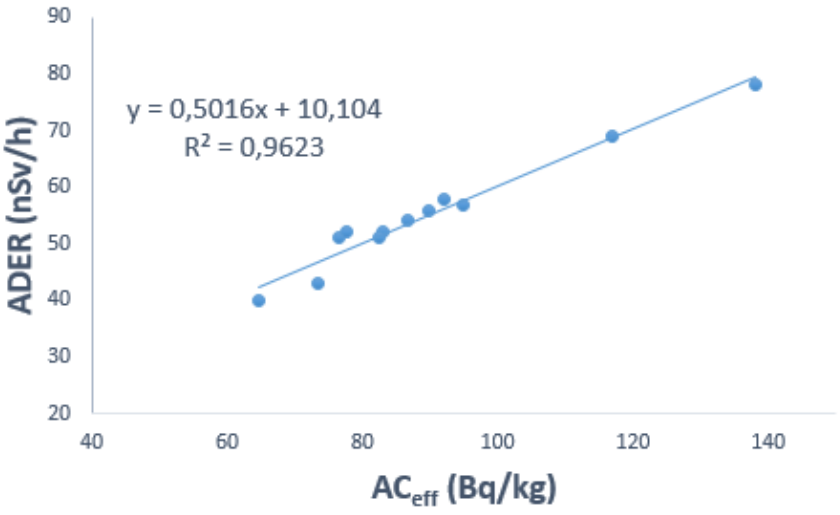

Figure 12: Calculated conversion coefficient by regression analysis of AC_{eff} and ADER.

Table 8 and 9 display $ADER_{total}$ and AC_{eff} obtained by the instrument from measurements at 0.1 meter and 1 meter respectively for each site. $ADER_{NORM}$ and $ADER_{ant}$ were calculated using equation 2.11 and 2.13 respectively. Notice that the sum of $ADER_{NORM}$ and $ADER_{ant}$ is 5 nSv/h lower than $ADER_{total}$. This is because of the sum of the cosmic component and intrinsic noise of the detector having this value.

Table 8: Measurement results of the spectrometer-dosimeter at 0.1 m distance from the ground.

Site	$ADER_{total}$ (nSv/h)	AC_{eff} (Bq/kg)	$ADER_{NORM}$ (nSv/h)	$ADER_{ant}$ (nSv/h)	$ADER_{ant}$ input to ADER (%)
1	53	82 ± 10	41	7	14
2	58	92 ± 11	46	7	13
3	52	83 ± 9	42	5	12
4	43	74 ± 8	37	1	3
5	78	138 ± 13	69	4	5
6	51	77 ± 8	38	8	16
7	54	87 ± 9	44	5	11
8.1	87	163 ± 15	82	0	0
8.2	62	101 ± 12	51	6	11
9	62	94 ± 10	47	10	17
10	42	55 ± 6	28	9	26

Table 9: Measurement results of the spectrometer-dosimeter at 1 m distance from the ground.

Site	$ADER_{total}$ (nSv/h)	AC_{eff} (Bq/kg)	$ADER_{NORM}$ (nSv/h)	$ADER_{ant}$ (nSv/h)	$ADER_{ant}$ input to ADER (%)
1	52	80 ± 10	40	7	14
2	57	95 ± 11	48	4	8
3	51	82 ± 9	41	5	10
4	40	65 ± 8	32	3	7
5	69	117 ± 12	59	5	8
6	56	90 ± 10	45	6	12
7	52	78 ± 9	39	8	17
8.1	61	109 ± 11	55	1	2
8.2	65	89 ± 12	45	15	25
9	67	109 ± 11	55	7	12
10	41	53 ± 6	27	9	26

4.1.3 Soil samples

Activity concentration measured in soil samples using high-resolution gamma spectrometry in the laboratory is shown in Table 10. Each assessed radionuclide is accompanied by a corresponding detection limit (MDA). ^{60}Co is not included in the table since it did not exceed the MDA at any sites except site 9. There, ^{60}Co was detected at a depth of 0-5 cm and the activity concentration was 1.25 ± 0.28 Bq/kg while MDA was 0.88 Bq/kg.

Table 10: Activity concentration (dry weight) and MDA for the assessed radionuclides (Bq/kg) with a coverage factor of k=1.

Site	Date	Sample Description(cm)	^{226}Ra		^{40}K		^{228}Ac		^{137}Cs		Detector
			A	MDA	A	MDA	A	MDA	A	MDA	
1	2021-09-14	Surface layer	123 ± 11.7	44.7	695 ± 21.8	45.4	13.8 ± 2.1	7.8	13.2 ± 0.8	2.9	4
		0-5 cm	20.9 ± 4.1	16.2	740 ± 20.8	16.6	18.0 ± 1.3	2.8	14.7 ± 0.5	1.0	5
		5-10 cm	<MDA	26.2	818 ± 26.2	23.0	11.8 ± 1.7	3.7	8.5 ± 0.5	1.3	7
		10-15 cm	<MDA	13.6	795 ± 22.2	14.0	12.0 ± 0.9	2.4	3.7 ± 0.3	0.9	5
		15-20 cm	48.9 ± 5.9	23.9	764 ± 21.2	24.3	8.4 ± 1.1	4.2	< MDA	1.5	4
2	2021-09-14	Surface layer	71.1 ± 8.5	33.7	592 ± 18.4	34.2	16.8 ± 1.7	5.9	3.6 ± 0.5	2.2	4
		0-5 cm	<MDA	15.6	691 ± 19.5	16.0	22.0 ± 1.5	2.7	5.4 ± 0.3	1.0	5
		5-10 cm	40.0 ± 9.1	31.7	708 ± 23.3	27.8	20.1 ± 2.4	4.5	5.8 ± 0.5	1.6	7
		10-15 cm	29.6 ± 4.3	14.2	564 ± 22.9	13.3	16.8 ± 1.3	2.2	4.6 ± 0.3	0.8	4
		15-20 cm	<MDA	27.3	742 ± 24.0	24.0	20.5 ± 2.4	3.9	5.3 ± 0.4	1.4	7
4	2021-09-14	Surface layer	87.0 ± 8.2	30.2	430 ± 13.7	30.7	7.6 ± 1.4	5.3	3.9 ± 0.5	1.9	4
		0-5 cm	<MDA	15.5	493 ± 14.3	15.9	16.5 ± 1.2	2.7	4.4 ± 2.8	1.0	5
		5-10 cm	<MDA	12.2	532 ± 15.0	12.5	16.0 ± 1.1	2.1	3.9 ± 0.2	0.8	5
		10-15 cm	42.2 ± 8.7	28.4	539 ± 18.1	25.0	16.0 ± 2.0	4.0	4.2 ± 0.4	1.5	7
		15-20 cm	<MDA	26.2	573 ± 18.9	23.0	17.2 ± 2.1	3.7	4.6 ± 0.4	1.3	7
5	2021-10-12	Surface layer	<MDA	17.2	592 ± 17.0	17.7	20.2 ± 1.4	3.0	<MDA	1.1	5
		0-5 cm	<MDA	15.4	603 ± 17.2	15.8	20.8 ± 1.4	2.7	<MDA	1.0	5
		5-10 cm	<MDA	25.5	682 ± 22.1	22.4	20.4 ± 2.4	3.6	<MDA	1.3	7
6	2021-10-12	Surface layer	75.5 ± 8.2	31.3	613 ± 18.4	31.7	13.6 ± 1.7	5.5	6.3 ± 0.5	2.0	4
		0-5 cm	<MDA	11.8	720 ± 20.0	12.2	25.2 ± 1.6	2.1	5.9 ± 0.3	0.8	5
		5-10 cm	41.8 ± 8.1	24.5	828 ± 26.4	21.5	24.6 ± 2.8	3.5	4.4 ± 3.9	1.3	7
7	2021-10-12	Surface layer	100 ± 8.4	28.2	448 ± 14.7	28.6	11.5 ± 2.0	7.7	11.1 ± 0.5	1.8	4
		0-5 cm	<MDA	10.9	583 ± 16.2	11.2	20.6 ± 1.3	1.9	12.8 ± 0.4	0.7	5
		5-10 cm	<MDA	9.0	639 ± 17.6	9.2	19.0 ± 1.2	1.6	10.0 ± 0.3	0.6	5
9	2021-10-12	Surface layer	181 ± 11.5	20.5	764 ± 20.6	20.8	40.6 ± 2.6	3.6	9.9 ± 0.5	1.3	4
		0-5 cm	71.2 ± 5.2	10.1	801 ± 22.1	10.4	61.6 ± 3.6	1.8	11.5 ± 0.4	0.7	5
		5-10 cm	73.8 ± 9.6	18.0	817 ± 25.7	15.8	56.7 ± 6.0	2.5	5.9 ± 0.3	0.9	7

Graphs of the activity concentration of ^{137}Cs in soil samples are displayed in Figure 13, in samples taken inside and outside the fence of Barsebäck NPP.

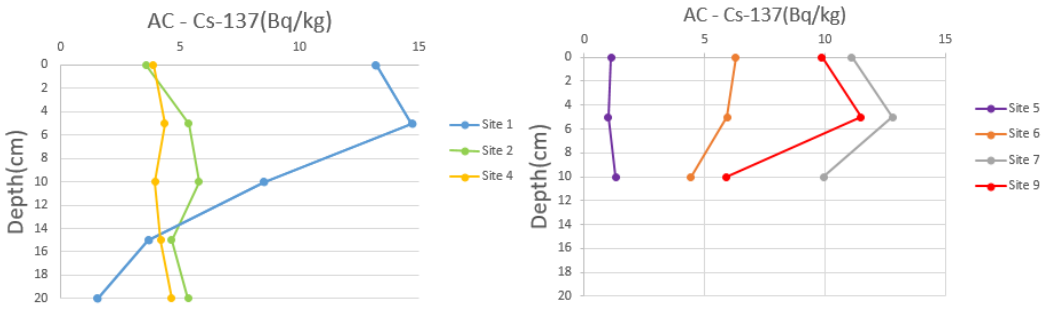

Figure 13: ^{137}Cs activity concentration (AC) at various depths in the different sites. Left figure shows soil samples taken at sites outside the fenced area. The figure to the right show soil samples taken at sites located inside the fenced area.

According to reports, the dry weight (dw) activity concentration of pond A contained a maximum of 12 Bq/kg ^{60}Co. However, only three out of ten locations contained a value above MDA and this value was between 3.6-8.3 Bq/kg. ^{137}Cs in pond A had an average activity concentration of 51 Bq/kg. Pond V contained an average of 162 Bq/kg ^{60}Co and 27 Bq/kg ^{137}Cs, where maximum was 493 Bq/kg and 60 Bq/kg respectively. All the ^{60}Co contamination is linked to the NPP activities[8, 27]. This is not the case for ^{137}Cs, instead the contamination is only partly linked to the activities of the NPP where the other part is due to atmospheric fallout.

4.1.4 Mobile gamma spectrometry

Figure 14 display a map of Barsebäck NPP and the mobile gamma spectrometry car measurement. SDI-dose rate from the measurement was converted to ADER and below the figure is a color coded ADER is shown.

Figure 14: Car-borne mobile gamma spectrometry measurement with color coded ADER.

A few locations are orange colored suggesting a slight elevation in the dose rate.

In Figure 15 all backpack measurements performed with mobile gamma spectrometry are displayed. These measurements covered all sites and additional areas close to the sites located inside the fenced area. Also, the restricted area of the NPP was also covered with backpack measurements.

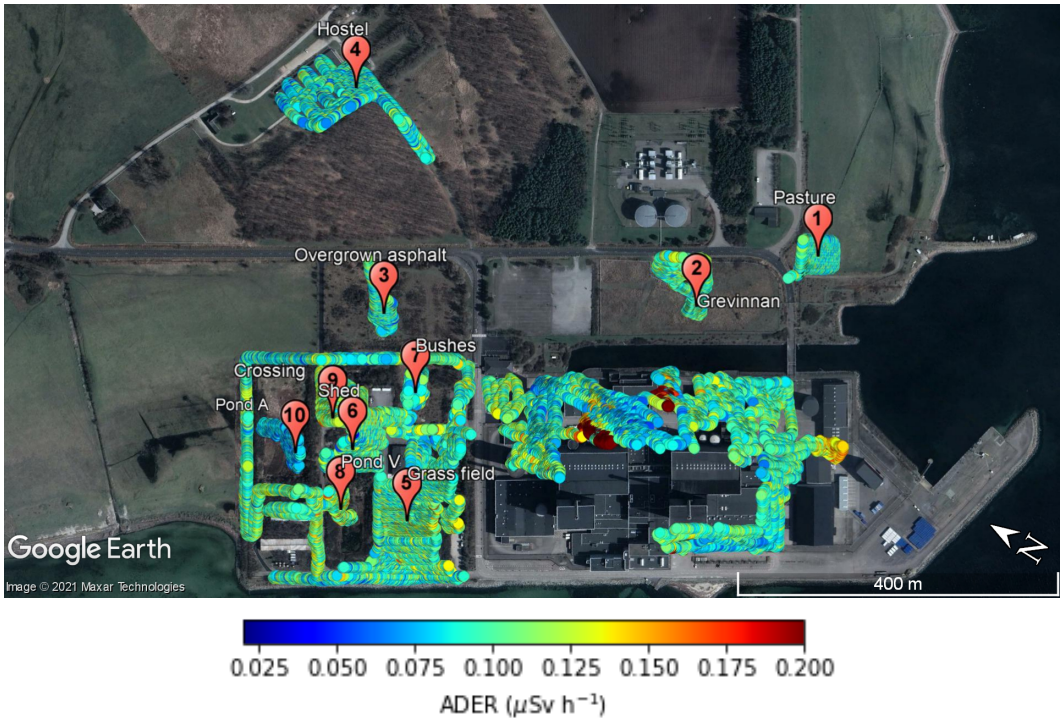

Figure 15: Mobile gamma spectrometry including all areas covered with backpack measurements.

Figure 15 gives an overview of the ADER levels in the area but a closer look on the backpack measurements outside the fenced area can be seen in Figure 16.

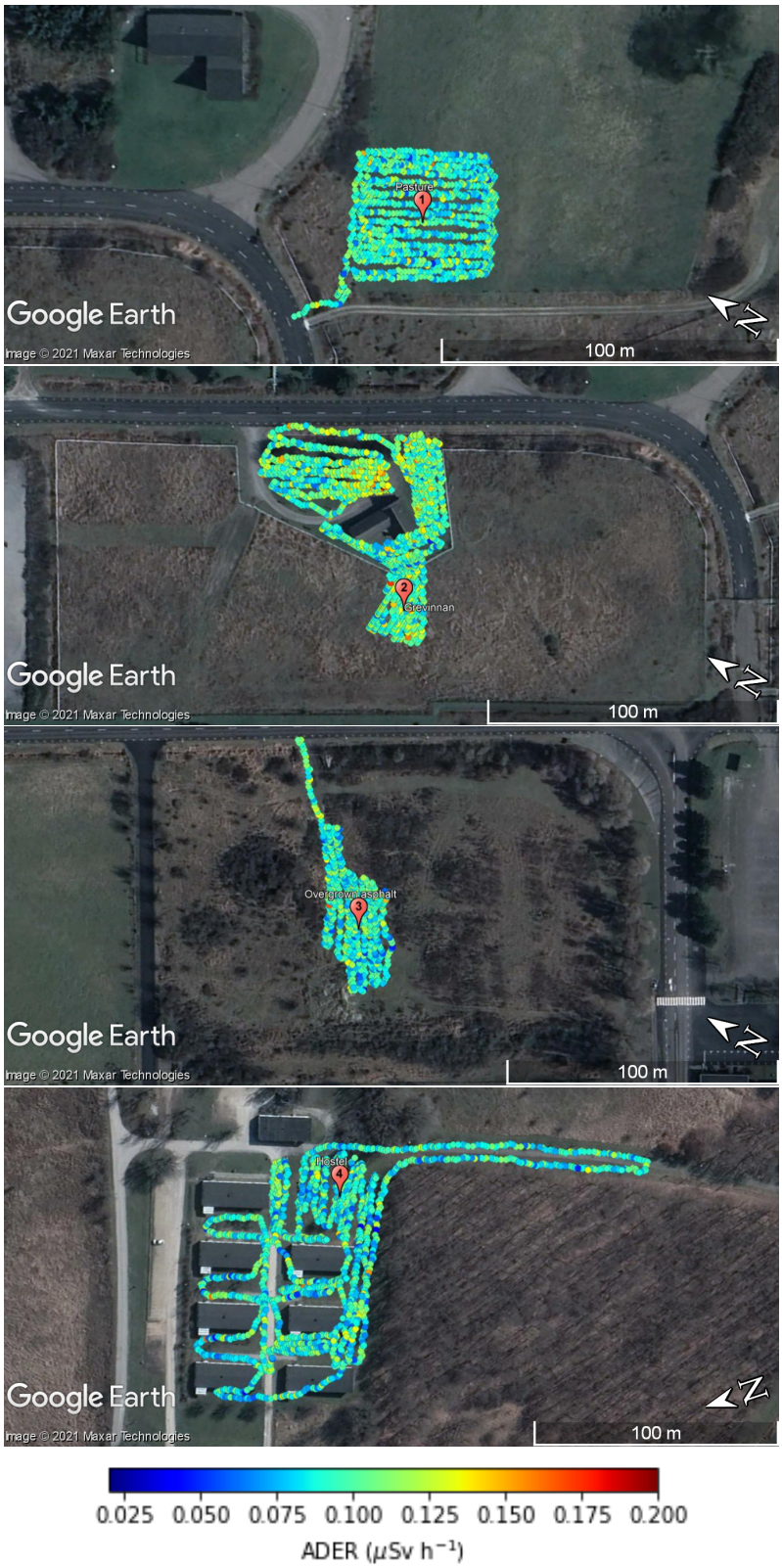

Figure 16: Mobile gamma spectrometry outside the fenced area (sites 1-4) covered with backpack measurements.

A close up version of the individual sites inside the fenced area is shown in Figure 17 and 18.

Figure 17: Mobile gamma spectrometry inside the fenced area (sites 5-7) covered with backpack measurements.

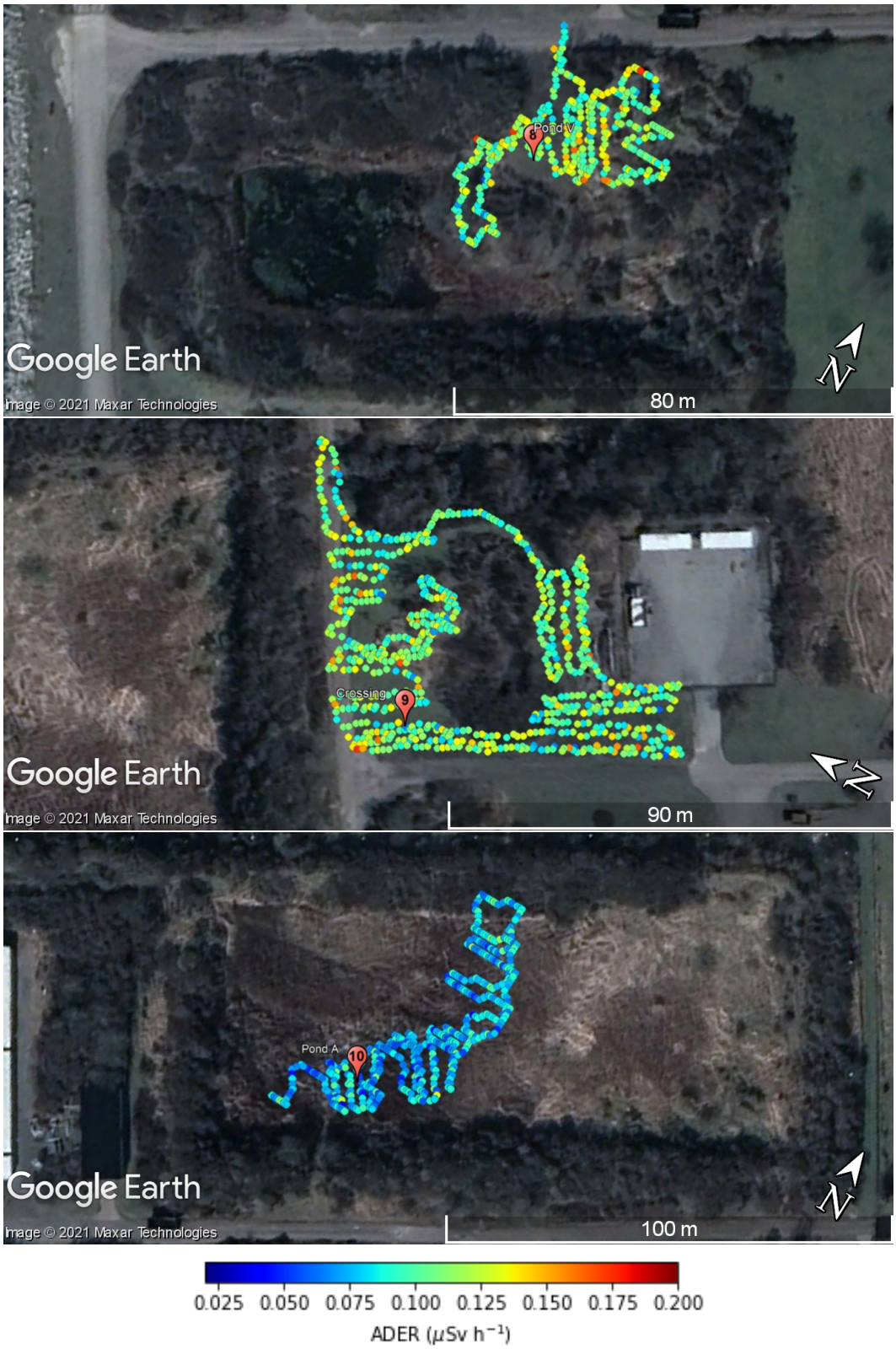

Figure 18: Mobile gamma spectrometry inside the fenced area (sites 8-10) covered with backpack measurements.

Mobile gamma spectrometry backpack measurements in the restricted area at the NPP is shown in Figure 19.

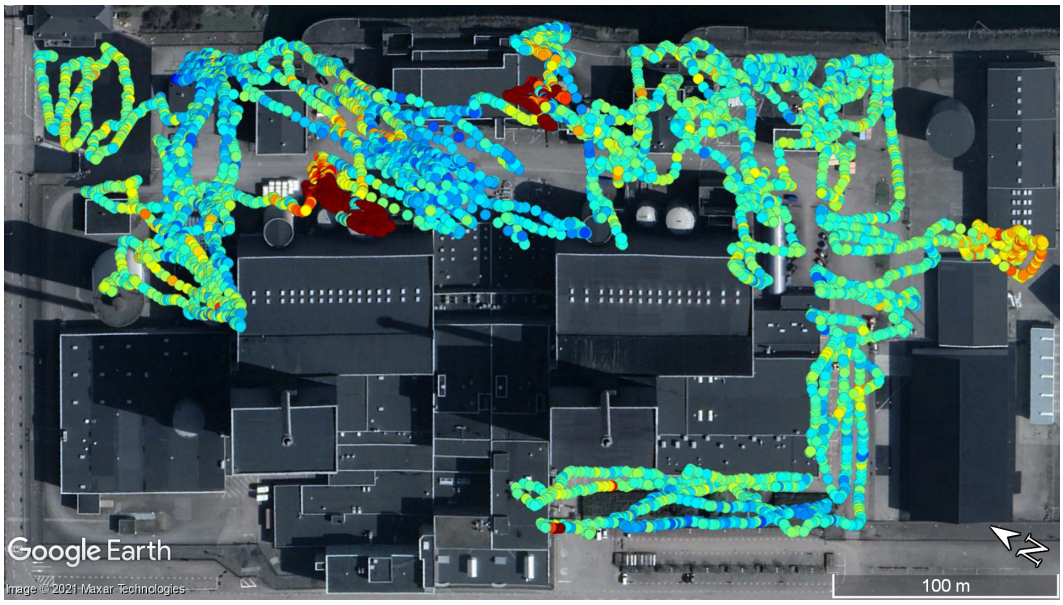

Figure 19: Mobile gamma spectrometry inside the restricted area covered with backpack measurements.

In Figure 19, it is possible to distinguish areas where ADER were elevated, up to a factor of 100 as compared to the average SDI dose rate outside the fenced area. The ADER level even exceed the scale at two locations, one outside the liquid waste management building and the other area is close to the B2 turbine building, in the vicinity of the discharge tanks. These areas measured a maximum SDI-dose rate of 0.3 µSv/h and 5.96 µSv/h respectively, exceeding the color scale having a maximum of 0.2 µSv/h.

Table 11 and 12 show SDI-dose rate values from each site and ID. Backpack measurements at and close to site 1-10 had an average SDI-dose rate of 58 nSv/h excluding the car measurement. Outside the fenced area the average value was 57 nSv/h, while inside the fenced area the average was 59 nSv/h. The restricted area had an altogether higher SDI-dose rate, the average was 124 nSv/h. ID 13 and 14 had the largest SDI-dose rate because of two areas where contamination was present and known before the measurement was carried out.

Table 11: Average (Avg.) SDI-dose rate measured using the backpack on all sites and the car measurement on roads.

Site/ID	Avg(nSv/h)	Std dev(%)
1	60	18
2	59	19
3	56	18
4	53	20
5	60	18
6	57	18
7	56	20
8	63	18
9	61	18
10	54	19
16	53	19
17	57	18
18	56	19
19	56	18
Car	88	19

Table 12: Average (Avg.) SDI-dose rate measured using the backpack in the restricted area.

Site/ID	Avg(nSv/h)	Std dev(%)
11	74	23
12	68	16
13	91	47
14	321	244
15	67	19

4.2 Ambient dose equivalent rate

Ambient dose equivalent rate measured with the handheld radiation protection instrument at each site is presented in Table 13 along with uncertainty.

Table 13: ADER measurements results at each site.

Site	Max dose rate (nSv/h)	Min dose rate (nSv/h)	Avg dose rate nSv/h	Std dev(%)
1	103	85	94	8
2	107	98	102	4
3	101	86	92	7
4	75	69	73	4
5	110	104	108	3
6	102	90	96	5
7	99	90	93	4
8	122	97	111	11
9	127	100	110	9
10	88	71	77	9

Outside the fenced area, average dose rate was 90 nSv/h while inside the fenced area, dose rate was on average 99 nSv/h. Average dose rate across all sites was 95.6 nSv/h.

Chapter 5

Discussion

5.1 Gamma spectrometry

5.1.1 Assessments using a HPGe detector

In situ gamma spectrometry using the HPGe detector showed surface activity that correlates well with earlier measurements of the area, made in 2012[28]. Results from earlier radiological characterization of Barsebäck NPP showed surface activity of ^{137}Cs between 0.2-0.5 kBq/m^2. In this report, most of the sites measured have similar results and the sites with the highest detected levels were sites 9 and 10, having ^{137}Cs contamination of 569 Bq/m^2 and 719 Bq/m^2 respectively. These sites measured a larger ^{137}Cs activity concentration than the theoretical decay corrected value of 0.52 kBq/m^2. It was expected that site 10 would have increased concentration of ^{137}Cs due to radioactive sediment being placed there years ago. At site 8 (pond V), it was expected that ^{137}Cs surface activity would be above average for the entire Barsebäck area investigated, since the largest quantity of radioactive sediment was placed there. This was not the case however, as it turned out to be relatively low (68 Bq/m^2) compared to the other sites. This can be explained by the position of the HPGe detector during measurement. Pond V contains a large amount of vegetation making it difficult to cover the pond itself with a measurement and ^{137}Cs is not homogeneously distributed across the pond. The measurement took place atop of a hill at a plateau covered with small rocks and not directly positioned on the pond which was the case for pond A. Below this hill was the pond with vegetation surrounding. Also, the pond is water filled, which functions as an effective radiation shielding material.

The lowest ^{137}Cs surface activity, 39 Bq/m^2, was found at site 3. A plausible reason for this low value is that the hard surface of site 3 is probably asphalt and possible contamination, originating from wet- and dry deposition, have been relocated elsewhere during precipitation and other weather conditions. ^{137}Cs from external anthropogenic sources may also be buried beneath the asphalt depending on when it was constructed. Earlier radiological characterization of asphalt and concrete surfaces measured ^{137}Cs surface activity of approximately 0.1 kBq/m^2 which means that this is an expected result. The calculation of surface activity involved an efficiency calibration of the detector that anticipated a fresh fallout, assuming a few centimeters of activity penetration in the soil. As seen in soil samples this is not a correct assumption since there is activity deeper in the soil from anthropogenic radionuclides. However, this efficiency calibration is chosen over the homogeneous efficiency calibration, which is used for NORM radionuclides, as it is more optimal for the vertical distribution of anthropogenic radionuclides in the soil.

Measurements of ^{3}H and ^{14}C were not included in this report but data from earlier reports confirm that these radionuclides were at levels of the natural background[28]. The majority of the radioactive contamination that can be related to the activities of the NPP is located in the ponds. This can be concluded from Table 5 where sites 9 and 10 contain the most amount of ^{137}Cs and ^{60}Co. Site 8 is also included along with site 9 and 10 since it is well known through earlier studies that an increased amount of radioactivity is present although the results in this study do not display the magnitude. The inventory of the ponds consist of ^{137}Cs and ^{60}Co and it is estimated that approximately half of the Cs-137 originates from the Chernobyl accident and half from the Barsebäck NPP operations. To improve the radiological characterization done in 2012 it was suggested that other more sensitive equipment should be used. Among the suggestions, one was to use a HPGe detector instead of the NaI(Tl) detector that was used then. This allowed for improved quantification of anthropogenic radionuclides.

Considering the theoretical decay corrected contamination of ^{137}Cs from Chernobyl of 0.52 kBq/m^2 in 1986 at Barsebäck, it is deduced that there were no major contributions of contamination from the NPP itself to the surrounding area when comparing this value to those in Table 5. A reasonable assumption can be made that also here the contamination mainly originates from nuclear weapon tests and the Chernobyl accident. Instead the NPP contamination is rather concentrated in the ponds. There is a possibility of an increase in contamination on some surfaces within some areas due to historical events such as leakages of radioactive water from the waste treatment facility of the restricted area, where further measurements with *in situ* gamma spectrometry would be interesting. This would, however, require measurements where the HPGe detector is collimated in order to reduce the potential radiation contribution from the surrounding buildings.

The surface activity outside the fenced area of Barsebäck NPP showed ^{137}Cs levels that are in the same order of magnitude as inside the fenced area. ^{60}Co is not present naturally in earth and should therefore not be detected at any rate when performing measurement on an area that is not contaminated. In Table 5, ^{60}Co is present at most sites indicating contamination from the NPP. 70% of the sites contained ^{60}Co above MDA, where four of these sites (2, 5, 6 and 7) showed a very low activity concentration. Outside the fence, sites 1-4 gave interesting results. Site 2, which is closer to the NPP than the other sites, had a surface activity above MDA in contrary to the other sites outside the fence. At site 3 however, the hard surface lead to believe that radioactivity has dissipated through precipitation hence leading to not being able to detect any ^{60}Co there. Site 4, being the farthest away from the NPP of the sites measured, had such low surface activity of ^{60}Co that it did not exceed MDA. Inside the fence it can be concluded that site 6 contained the least amount of ^{60}Co and yet it is above MDA. The most likely case is that this site do not contain any ^{60}Co contamination as a conclusion drawn from observing the large uncertainty tied to this small measured value. The other sites show a presence of ^{60}Co, where site 10 contained the highest concentration (79 Bq/m^2) which was anticipated. Elevated levels are shown also at site 9 where no ^{60}Co was placed but it is geographically located close to the ponds. A possible reason for the contamination of these areas can be that when the ponds were built, dust particles and aerosols containing radionuclides filled the air and the wind transported these particles to respective site where they integrated with the surface causing contamination. These results are encumbered by large uncertainties and for many

of the sites where ^{60}Co were detected, it is more plausible that it actually comes from the nearby buildings rather than contaminations in the ground. This would explain why ^{60}Co in soil samples were below MDA at almost all sites. This hypothesis could also be verified in places where it is not possible to gather soil samples by carrying out a collimated measurement shielding the detector from radiation of nearby buildings.

The average ^{137}Cs surface activity across all sites was 280 Bq/m^2. Compared to measurements at ESS this is substantially larger, in fact by 142%[22]. Although there are factors to consider when discussing the magnitude of this amount. One factor is that the fallout from Chernobyl was unevenly distributed, meaning some areas will contain a large amount of ^{137}Cs while other areas will contain almost nothing. Hence, it is possible that Barsebäck received more ^{137}Cs than the area where ESS is built. Another factor to consider is that measurements were focused around and close to the two ponds where it is known that radioactivity has been placed recently. This is not the case for ESS as there is nothing of the sort and also the ground at ESS is recently placed from relocated deep layer soils and sediments. All factors are involved to some degree and must be considered when assessing whether or not this average activity concentration is a large value.

Regarding NORM radionuclides Table 4 display results that resembles the results of the Zero Point report around ESS. ^{40}K is represented with an average activity concentration of 408 Bq/kg compared to 407 Bq/kg at ESS. This result agrees very well with measurements at ESS and also with the average in the world which is 400 Bq/kg. ^{40}K vary over seasons, growing conditions and plant species. It can explain the low value compared to the average of Sweden (780 Bq/kg). The lowest value was at 197 Bq/kg while the highest value was 655 Bq/kg. The rather small amount of sites could contribute to source of error when considering the average value here even though it agrees well with the activity concentration reported from earlier measurements of the same region. ^{226}Ra and ^{228}Ac average values agrees well with the results from the ESS Zero Point report. ^{40}K has a small uncertainty, attributed by Poisson statistics, because of the high count. Also the high energy (1460 keV) provide less noise from Compton continuum of other radionuclides. ^{7}Be suffered from the problem of a large uncertainty. ^{7}Be has an energy of 487 keV and hence, noise is not so much of an issue there. Instead, its large uncertainty is due to the low counts generated.

5.1.2 Assessments using a spectrometer-dosimeter

Measurements with the spectrometer-dosimeter were carried out to investigate the amount of ADER originating from anthropogenic radionuclides. In general, the total ADER obtained was low compared to the ADER from the hand-held radiation protection detector measurements. For sites 1-4 the contribution from anthropogenic radionuclides was low as seen in Table 8 and 9. Lowest ADER was observed at site 4 which corresponded well with the HPGe measurement and soil sampling. Largest value was obtained at site 1. Contribution of anthropogenic radionuclides were 14%, both at 0.1 m and 1 meter respectively, of the total ADER.

Among the sites inside the fenced area, site 5 and 8.1 had the lowest contribution from anthropogenic radionuclides to the ADER. For site 5, this agrees well with the other measurements, for instance the results from soil samples which was

below MDA. At site 8, an additional measurement was carried out. In Table 8 and 9 this location was called 8.2. Comparison between the measurements at site 8 display the variation in $ADER_{ant}$ between the different locations. Site 8.2 was located as close as possible to the water of pond V. In both cases: 0.1 meter and 1 meter, site 8.2 had a larger contribution from anthropogenic radionuclides to the ADER compared to site 8.1. Sites 6, 7, 8.2, 9 and 10 all showed large contribution from anthropogenic radionuclides, with sites 7, 8.2 and 10 having the largest contribution in percent of the total ADER at 1 meter measurement. While sites 6, 9 and 10 had the largest contribution at 0.1 measurements.

5.1.3 Soil samples

Many soil samples collected from sites were close to MDA for ^{226}Ra. This suggest that the ground in general was deficient in ^{226}Ra. The average activity concentration for those samples that were above MDA was 71.9 Bq/kg. This is more than twice the magnitude acquired with *in situ* gamma spectrometry. The statistical estimation was however more accurate in the measurements of the soil samples and hence this result is more reliable than the *in situ* gamma spectrometry measurement.

In the majority of sites the ^{137}Cs activity concentration was above the MDA. There were two cases where this was not true however, in sites 1 and 5. For site 1, this only occurred at a depth of 15-20 cm. A reasonable explanation is that collection of soil samples at this site was increasingly difficult as a function of depth. At 15-20 cm a large part of the ground consisted of rocks. This lead to a reduced amount of soil being gathered of this particular depth. Thus, a 60 ml geometry had to be used. Looking at Figure 13 it is possible to see that activity concentration at site 1 is decreasing as a function of depth starting from 5 cm. This makes it plausible that at a depth of more than 15 cm at site 1 there is a low ^{137}Cs activity concentration which cannot be detected. Soil samples inside the fence in Figure 13 display one discrepancy, namely site 5. The activity concentration in this site was substantially less than site 6, 7 and 9. All soil samples at site 5 were below MDA, hence, there were no detectable amounts of ^{137}Cs at any of the depth measured. This can be explained by the penetration depth of ^{137}Cs being rather shallow. If the top layer of site 5 has been scratched clean and put elsewhere after 1986 it is possible that much of the ^{137}Cs was displaced. Or another possibility is that the ground at site 5 has been covered with new layers of soil after 1986, which would also give these results.

The average ^{137}Cs activity concentration across the sites where the value was above MDA was 7 Bq/kg. This is not so surprising considering the Chernobyl accident and nuclear weapon tests. Activity concentration in these sites resemble the results obtained in the Zero Point report where measurements were performed at ESS in Lund. Figure 13 show that site 1 contained more activity than sites 2 and 4. It also shows that sites 7 and 9 holds an increased amount ^{137}Cs compared to sites 5 and 6. This agrees well with the *in situ* gamma spectrometry that was performed with the HPGe detector. The proportionality between activity concentration and surface activity is apparent here since sites with a large activity concentration, such as site 1, also had a large surface activity. Figure 13 show that at sites 2 and 4 the ^{137}Cs activity concentration does not vary significantly with depth. Although it is possible to see that the highest activity concentration is at the depth of 0-5 cm.

This is true in almost all cases presented, where site 6 is an exception. Depth variations of ^{137}Cs can be visually interpreted using site 1 as a reference. At 10-15 cm the activity concentration is about the same as sites 2 and 4. Reaching 5-10 cm, the activity concentration is increasing more than at the two other sites. Then it dramatically increase, even more at 0-5 cm, and when reaching the surface layer it reduces somewhat. At 0-5 cm the value at site 1 was 14.7 Bq/kg which was the largest activity concentration registered. Site 1 containing the most ^{137}Cs agrees well with the highest value measured at ESS which was of the same magnitude, 17.8 Bq/kg. Although these are elevated levels of ^{137}Cs, they are not alarming in any way, but rather normal variations between different locations.

The result from soil sample measurements indicate that the ^{60}Co levels are below the MDA values at the Barsebäck NPP area. There was only one soil sample exceeding MDA, with a very low activity concentration at site 9. In this work, there were no soil samples acquired at sites 8 and 10. Fortunately, a recent report was made concerning the two ponds at these sites. Dry weight soil samples were collected and the ^{60}Co activity concentration at site 10 was low, most samples did not exceed detection limits. At site 8, where activity concentration of ^{60}Co was higher, it was found that the top layer (0-10 cm) had the highest activity concentration. This is in accordance with the results in this study.

5.1.4 Mobile gamma spectrometry

Mobile gamma spectrometry, where either backpack or car measurements were performed showed to be of great value in characterizing the radiation environment in the area of Barsebäck NPP. The benefit of using the mobile methods was the usefulness to pinpoint locations of interest. In addition, it could also assess the radiation exposure at each coordinate. Using the excel file of data created, the maximum dose in the area could be extracted as well as the average over the given area. However, SDI-dose rate is a rough estimate of ADER and its values should rather be viewed as a qualitative characterization of variations in the radiation environment. It is merely a tool to survey areas for contamination so that other methods can be applied for further assessment of the radiological environment. Cross calibration of SDI-dose rate with a measured average ADER enabled conversion of SDI-dose rate to ADER. This was implemented as an attempt to visualize the radiological characterization of each mobile gamma spectrometry measurement and Figures 14-19 are all displaying dose rate in ADER. The SDI-dose rate data was divided into two separate tables, where Table 11 focus on measurements done inside and outside the fenced area of the NPP and Table 12 shows the measurements made in the restricted area. Results from Table 11 display average SDI-dose rates between 53 and 63 nSv/h. Average across all sites was 57 nSv/h which is substantially less than that of a normal background dose rate. Normal background dose from external radiation in Sweden is approximately 0.9 mSv/y from radiation sources, excluding medical examinations, this gives a calculated dose rate of approximately 100 nSv/h[6]. The contribution to dose rate from different radionuclides is not qualitatively analyzed in the mobile gamma spectrometry. But it is safe to say that even though there has been anthropogenic radionuclides identified with HPGe measurements in a number of sites the dose rate from these radionuclides is not large enough to exceed the dose limit. If the dose limit is exceeded, measurements are needed to quantify the dose rate of these radionuclides to assess if they

contribute more to the dose than what is allowed. The car measurement gave reason to believe that there were two more locations where the dose rate was elevated. One location was outside a storage building where parts from the reactor is temporarily stored and the other location was outside a building where measurements are performed on containers containing radioactive waste. A suggestion is to evaluate these locations further with a calibrated instrument such as the scintillation probe. If an elevated dose rate is observed, complementary measurements could be performed with *in situ* gamma spectrometry.

Table 12 contain the average SDI-dose rate for the sections in the restricted area. The average SDI-dose rates of ID 12 and 15 are similar to the SDI-dose rates outside the restricted area in Table 11 and can thus be discarded as potential risk zones of radiation hazard. At site 11, the average SDI-dose rate was elevated because of two locations where the SDI-dose rate was increased. These two locations were at the entrance to reactor B1 and close to the temporary storage building where parts from the reactor are stored. ID 13 and 14 contained locations where the SDI-dose rate was significantly increased (red dots in Figure 19). In one of the locations there was a leakage of contaminated water from the waste building in 2020, contaminating the asphalt surface outside the building. This is located at the inlet of the cooling water and the other location is close to the turbine building of B2. There is an interest to examine these areas of elevated dose rate levels in the restricted area further by conducting more accurate dose rate measurements and *in situ* gamma spectrometry to identify possible radionuclides present as well as quantification of these.

5.2 Ambient dose equivalent rate

In Table 13, results from the ADER measurements show values around 100 nSv/h for all sites. Sites 4 and 10 had lower values, 75 nSv/h and 88 nSv/h respectively. The low value at site 10 can be due to the ground being covered by water from recent precipitation before the measurement was carried out. The water function as shielding against radiation and since site 10 is an enclosed pond, water will stay in the area until warmer weather allows it to evaporate. Sites 5, 8 and 9 had the highest values of ADER, exceeding the typical background dose rate. At most it exceeds normal background by 11%, although, small increases like this is probably due to fluctuations. Site 5 had, according to the *in situ* gamma spectrometry measurement (Table 5), the lowest activity concentration of anthropogenic radionuclides inside the fenced area and yet the ADER was larger than 100 nSv/h. Hence, it depends on something else, possibly fluctuations caused by the variations in NORM radionuclides. At sites 8 and 9 it is, however, more likely that the increase depends on anthropogenic radionuclides since it was discovered that there were a higher activity concentration at these sites. For site 8, it is not shown clearly with the *in situ* gamma spectrometry but in the measurement for anthropogenic ADER with spectrometer-dosimeter it was more obvious (see Table 9). There, a measurement was carried out at another location at site 8, this location was named 8.2. The difference between 8.1 and 8.2 is in well accordance with the standard deviation of the ADER measurement which experienced a relatively large deviation among the different positions at the site. Although, a slight increase in ADER, the results are not alarming in any way. Looking at the average inside and outside the fenced area,

we see that both are even below 100 nSv/h. It can be argued that more measurements would be needed to ensure these results are valid, in this work there were 42 ADER measurements carried out at 10 different sites.

Chapter 6

Conclusion

With the work effort put in this report the NORM and anthropogenic radioactivity has been characterized in the area surrounding the Barsebäck NPP both inside the fenced area and outside. The result from analysis of the measurements showed that anthropogenic radioactivity at the measurement points is in the same order of magnitude in the surroundings of the NPP. Hence, this strongly indicates that the NPP has not contributed to elevate the contamination levels above those originating from external contamination *i.e.* the Chernobyl accident and nuclear weapon tests.

Mobile gamma spectrometry covered a large area around the NPP with backpack and car-borne measurements. At sites 1-10 there were no significant increase in SDI-dose rate. However, backpack measurements revealed elevated levels of radiation in sections of the restricted area of the NPP which is attributed to contributions from building structures in the vicinity of the measurement locations. These sections were outside the liquid waste facility and outside of the turbine building of B2 close to the water discharge tanks.

In situ gamma spectrometry with HPGe detector discovered that surface activity of ^{137}Cs were, because of the low activity, in large part due to the Chernobyl accident and nuclear weapon tests. Site 8 and 10 were known to harbour an increased amount of anthropogenic radionuclides where contaminated sediments were put, from dredging of the Barsebäck basin and cleaning of the cooling water outlet. ^{137}Cs surface activity were somewhat elevated at sites 9 and 10. ^{60}Co were around the detection limits and were associated with large uncertainties. The reason for the low ^{137}Cs value at site 8 was due to the hard surface at that site. Closer to the water of pond V the anthropogenic radiation was higher which was discovered when carrying out an additional measurement using the spectrometer-dosimeter. Site 9 was of particular interest as the anthropogenic radiation were slightly elevated.

Results from soil samples showed that ^{137}Cs activity concentration were in the same order of magnitude, where the highest levels were detected at sites 1, 7 and 9. Soil samples were not taken at sites 8 and 10 but were confirmed in a recent report of having activity concentrations that exceed the rest of the sites[10]. This was also the case for ^{60}Co since all sites had activity concentrations below MDA with a single exception at site 9, where the value exceeded MDA by a small amount. The single soil sample at site 9 which had activity concentration above MDA was lower than those of sites 8 and 10.

The anthropogenic radionuclide contribution to ADER was measured at each site with the spectrometer-dosimeter. Results show that contribution in percent

was highest at sites 8 and 10. This was in good agreement with the results from the other measurement methods.

ADER measurements indicated that current dose rate at each site was around normal background. A few sites averaged above 100 nSv/h but it is more plausible to depend on fluctuations in activity from NORM radionuclides than activity from anthropogenic radionuclides.

Although this work consisted of a limited amount of measurements due to the fact that a comprehensive measurement of the area would require a larger workforce and/or more time, the activity levels of the identified gamma ray emitting radionuclides were generally relatively low or around the detection limits and the results can be used in the future when clearance of the site will be conducted. Hence this work is provided as a basis, to use as reference, for other radiation measurements and radiological characterization of the area around Barsebäck.

Bibliography

[1] SSM, [Internet], cited: 2021-11-09, <https://www.stralsakerhetsmyndigheten.se/omraden/karnkraft/avveckling-av-karntekniska-anlaggningar-i-sverige/>

[2] Swedish Nuclear Fuel and Waste Management Co. Kärntekniska industrins praxis för friklassning av material, lokaler och byggnader samt mark. December 2011. (In swedish)

[3] Gilmore, G. Practical Gamma-ray Spectrometry 2nd Edition. Nuclear Training Services Ltd Warrington, UK. John Wiley & Sons Ltd. 2008.

[4] Kock, P. Orphan source detection in mobile gamma-ray spectrometry. Lund University. 2012.

[5] Finck, R. High resolution field gamma spectrometry and its application to problems in environmental radiology. Lund University. 1992.

[6] Andersson, P, et.al. The radiation environment in Sweden. Statens strålskyddsinstitut. SSI report: 2007:02 january 2007. (In swedish)

[7] UNSCEAR 2000 report Vol. I. Sources and effects of ionizing radiation. 2000.

[8] Håkansson, L, 12460 - Projekt KAKA - Sammanställning av kontamination i jord, grundvatten och sediment på Barsebäcksverkets industritomt. BKAB report 2129512/3. 2018-01-22. (In swedish)

[9] Ranebo, Y, Radionuklider i sedimentdammar vid Barsebäcksverket 2014. BKAB report B1022573/0. 2014-01-10. (In swedish)

[10] Ören, Ü, Radiological assessment of pond sediments at the Barsebäck NPP site. BKAB report 1044483/0. 2021-12-23.

[11] IAEA - International Atomic Energy Agency, 2003. Guidelines for Radioelement Mapping Using Gamma Ray Spectrometry Data. IAEA-TECDOC-1363

[12] Isaksson, M., Erlandsson, B., Linderson, M-J. Calculations of the deposition of 137Cs from nuclear bomb tests and from the Chernobyl accident over the province of Skåne in the southern part of Sweden based on precipitation. J. Environ. Radioactivity Vol.49, No.1, pp. 97-112 (2000).

[13] Nilsson, J. Mobile Gamma Spectrometry Development and optimisation of methods for locating and mapping lost radioactive sources. Medical radiation physics, Malmö. Lund University 2016.

[14] Persson, H, Detection limit concepts according to Currie, Mirion Technologies.

[15] Knoll, Glenn F. Radiation detection and measurement / Glenn F. Knoll Wiley New York, 1989.

[16] Lloyd A. Currie. Limits for qualitative detection and quantitative determination. Application to radiochemistry. Analytical Chemistry 1968. DOI: 10.1021/ac60259a007

[17] Radiation Dosimetry, [Internet], cited: 2021-11-09, <https://www.radiation-dosimetry.org/what-is-ambient-dose-equivalent-h10-definition/>

[18] Strålskyddsförordning (2018:506), [Internet], cited: 2021-11-09, <https://www.riksdagen.se/sv/dokument-lagar/dokument/svensk-forfattningssamling/stralskyddsforordning-2018506_sfs-2018-506>

[19] Harrison JD, Balonov M, Bochud F, Martin C, Menzel HG, Ortiz-Lopez P, Smith-Bindman R, Simmonds JR, Wakeford R. ICRP Publication 147: Use of Dose Quantities in Radiological Protection. Ann ICRP. 2021 Feb;50(1):9-82. doi: 10.1177/0146645320911864. PMID: 33653178.

[20] V.P. Ramzaev, A.N. Barkovsky, C. Bernhardsson, S. Mattsson. Calibration and testing of a portable NaI(Tl) gamma-ray spectrometer-dosimeter for evaluation of terrestrial radionuclides and ^{137}Cs contribution to ambient dose equivalent rate outdoors. 2017.

[21] Laraweb, [Internet], <http://www.nucleide.org/Laraweb/index.php>

[22] Bernhardsson, C, Stenström, K, Jönsson, M, Mattsson, S, Pedehontaa-Hiaa, G, Rääf, C, Sundin, K & Waldner, L 2019, Assessment of "Zero Point" radiation around the ESS facility. MA RADFYS 2018:01, BAR-2018/04, Lund University.

[23] Karlberg, O. Manual och teknisk beskrivning av CEMIK-systemet och NuggetOSM(version 4.0 rev 20). (In Swedish)

[24] Alan Proctor, Jeffrey Wellman, Exposure rate by the spectrum dose index method using plastic scintillator detectors, Radiation Protection Dosimetry, Volume 149, Issue 3, April 2012, Pages 309-314, https://doi.org/10.1093/rpd/ncr247

[25] Östlund, K. Methods for localizing and quantifying radionuclide sources and deposition using in situ gamma spectrometry : Critical review of the peak-to-valley method based on experimental studies and applications in Georgia and Japan. Lund University. 2017.

[26] Earth Point, [Internet], cited: 2021-10-01, <https://www.earthpoint.us/ExcelToKml.aspx>

[27] Adam, C., Garnier-Laplace, J., & Roussel-Debet, S. (2001). Radionuclide fact sheet: Cobalt and the environment. Irsn.

[28] Håkansson, L, Radiological Characterization of Barsebäck NPP. 2012-02-08. (In swedish)